CHARACTERIZATION OF BIOFUEL FROM DIATOMS VIA HYDROTHERMAL LIQUEFACTION

BY

PENG ZHANG

THESIS

Submitted in partial fulfillment of the requirements
for the degree of Master of Science in Agricultural and Biological Engineering
in the Graduate College of the
University of Illinois at Urbana-Champaign, 2014

Urbana, Illinois

Advisor:

Professor Yuanhui Zhang

ABSTRACT

Previous studies of hydrothermal liquefaction (HTL) converting low lipid content microalgae (*i.e.*, *Chlorella pyrenoidosa* and *Spirulina platensis*) have shown potential to utilize low lipid microalgae to produce bio-crude oil. Diatoms are a major group of microalgae in water bodies with a high growth rate and that contribute about 20% of global primary production. Their unique frustule (silica cell wall) results in a high ash content (39% dry weight). This character makes the bio crude oil absorbed in solid product after hydrothermal liquefaction, rather than viscous liquid product as we have seen from *C. pyrenoidosa* and *S. platensis*. Most of the organic matter in the diatom biomass was converted into alkanes, fatty acyls, and small fractions of undesirable nitrogen-containing compounds, such as pyrazines, according to GC-MS analysis. The inorganic frustules remained in the solid residue, unchanged after the hydrothermal process, with small amounts of organic matter attached, as revealed by SEM observation and FT-IR characterization. The higher alkane content indicated competitive quality of bio crude oil from diatoms to those from *C. pyrenoidosa* and *S. platensis*. However, challenges arise along with the high amount of solid residue, which may cause extra difficulty for product separation and reactor design.

ACKNOWLEDGMENTS

I would like to thank my advisor Dr. Yuanhui Zhang for his encouragement, support, and advice, without which this study could not have been accomplished. Dr. Zhang has put all his efforts into promoting the Environment-Enhancing Energy (E-2 Energy) concept, which integrates both wastewater treatment and biofuel production. I am very honored and proud to be one of the members in this research. I would also like to thank Dr. Lance Schideman and Dr. Brajendra Sharma for their valuable advice and serving on my defense committee.

Thanks to my fellow graduates and researchers, Wan-Ting Chen, Zhongzhong Zhang, Mitchell Minarick, Steve Ford, Dr. Guo Yu, Dr. Zhichao Wang, Dr. Yigang Sun, *et al*., in our group for their help and advice. It was really a great pleasure to work with them.

Last but not least, I cannot thank my family enough for their unconditional support and love.

TABLE OF CONTENTS

Chapter 1

Introduction

1.1. Energy Demand and Alternative Energy Sources

It is a simple fact that we are consuming more energy than ever before. Experts predict that the demand for energy will increase to 13,749 million tons of oil equivalent (Mtoe) by 2020, with an average annual increase of 2% (Birol and Argiri 1999). Admittedly there are many different energy sources, but fossil fuels (*i.e.*, petroleum, coal, and natural gas) represent the most widely used energy forms in today's market. In the United States as an example, fossil fuels comprise 83% of total energy consumption, while renewable energies and biofuels only 8% in 2010 (Figure 1.1). The remainder of the share (9%) is from nuclear energy (EIA 2012).

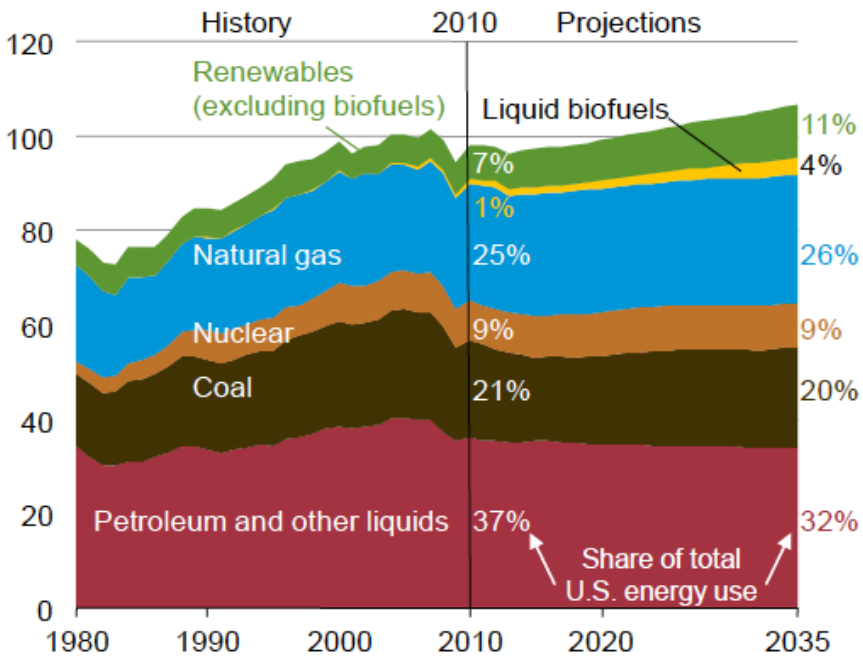

Figure 1.1 Energy Sources in United States from 1980 to 2035 (quadrillion Btu). The data after 2010 is estimated (EIA 2012)

Fuels for transportation are primarily from petroleum, and they take a share of about 1/4 of total energy consumption (IEA 2012). In next 15 years, the numbers of automobiles on the road will double to about 2 billion in the world, an explosion due primarily to increased consumer power in developing countries (Sperling and Gordon 2009). Thus, the demand for transportation fuels will most likely double as well.

Most of us agree that that oil reserves are not infinite. Having been deployed for so many years, petroleum production from the world's major oil fields have has begun to decrease. Experts estimate an average annual decline rate of 6.5% beyond this plateau phase. By the year 2030, these oil fields may well produce less than 50% of the oil that they yield today (Höök et al. 2009). In addition, several research models have predicted the peak of oil production would occur around the second decade of 21st century (Bentley and Boyle 2008; Bentley 2002).

How to meet the increasing energy demand with decreasing fossil fuel production is a serious challenge for current generations. Emerging renewable energy technologies have offered some promising approaches to solve this problem. Among them, biofuel production technologies have gained much attention, as these practices produce liquid fuels that can serve as alternatives to petroleum products. Blending biofuels into petroleum fuels is one of the simplest and most widely used methods of utilization. Bioethanol and biodiesel have already been added to gasoline and diesel to reduce the consumption of respective fuels, with typical blending ratio (bioethanol/biodiesel to petroleum fuels) of 5%, 10%, and 15%. However, most of the feedstocks used to produce bioethanol and biodiesel are food or food sources. For example, the bioethanol produced

in Brazil (16,489 million liters, in 2005) and in the United States (16,217 million liters, in 2005) from sugarcane and corn respectively together accounts for 62% of the production worldwide (Goldemberg et al. 2008; Escobar et al. 2009). The corn-to-ethanol conversion efficiency is estimated to be between 2.7 gallons/Bushel (gal/bu) (or 0.4L/Kg) to 3.0 gal/bu (or 0.45L/Kg) (Donner and Kucharik 2008). That is to say, to produce 16,217 million liters ethanol from corn, 36 million tons of corn is needed with the highest conversion efficiency.

Of course, the huge demand of corn and sugarcane as well as other food sources has a heavy impact on the food prices and food security. According to data from USDA National Agricultural Statistics Service, corn prices from 2000 to 2012 (October) increased from 2.34 US Dollars per Bushel to 6.64 US Dollars per Bushel with inflation adjustment, which is almost tripled. The consumption of food for fuel drains resources from the market and inevitably causes food shortage, which is reflected by soaring prices.

1.2. Microalgae as Feedstock for Biofuel

To achieve fuel sustainability, then, it is necessary to avoid using food resources to produce biofuels. Third generation biofuels (microalgae based biofuel) is very promising and sustainable. Microalgae are regarded as a collection of unicellular microorganisms that are capable of photoautotrophy. This classification includes prokaryotes and eukaryotes (Johansen 2011). As shown in Figure 1.2, blue-green algae, or cyanobacteria, represent the prokaryotic microalgae and are more closely related to bacteria. One the other hand, green algae are more closely related to higher plants. Other microalgae types fall in between the two ends.

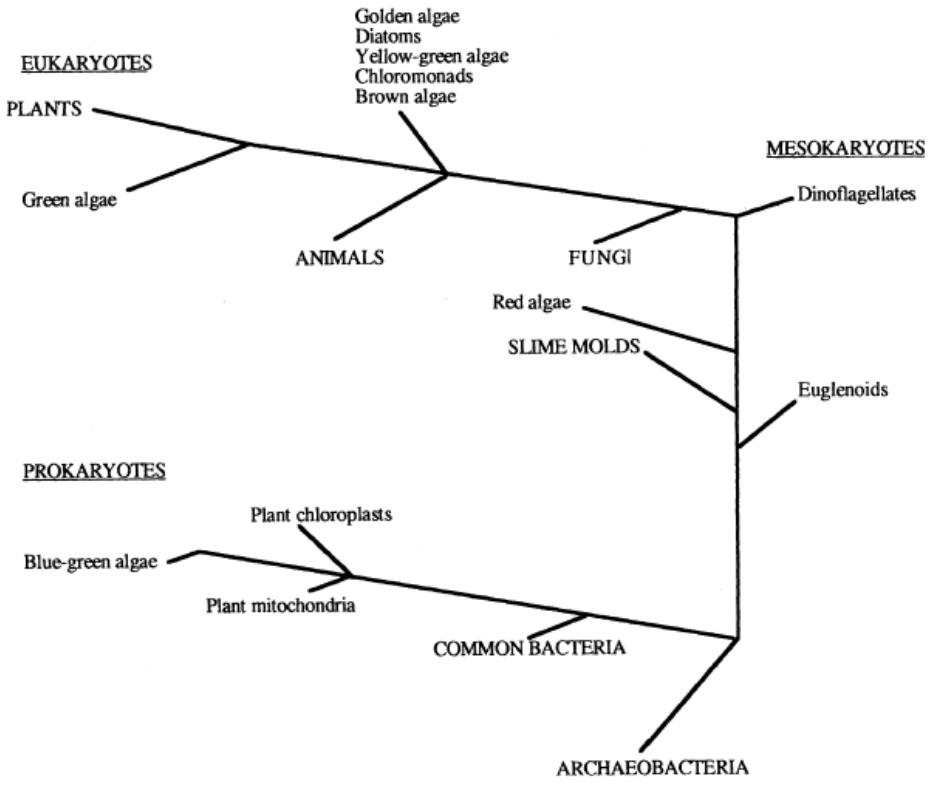

Figure 1.2 Phylogenetic classification of microalgae based on ribosomal RNA sequences (Radmer 1996).

Microalgae have a very high productivity (Table 1.1). They account for nearly half (46.2%) of annual global net primary productivity (NPP) with only 0.2% of global primary producer mass (Field et al. 1998). Among all the microalgae, diatoms, dinoflagellates, and coccolithophorids are prominent primary producers in modern oceans. It seems worth noting that diatoms alone contribute about 40% of the NPP in marine environment (Falkowski et al. 2004; Compton 2010), which makes diatoms worthy of study as a potential candidate feedstock for mass biofuel production. In addition, some species can survive even under extreme environmental conditions. For instance, two of the most well-known genera—*Spirulina* and *Dunaliella*—tolerate high alkalinity and high salinity, respectively, which makes them very good candidates for cultivation in arid areas as the underground water is likely to be alkaline or saline (Isichei 1990). The

development of mass production of microalgae has greatly improved productivity (Table 1.1), increasing the cost efficiency of microalgae production as well as microalgal biofuel production.

Table 1.1 Observed and projected yields for different crops including microalgae. Adopted from (Williams and Laurens 2010)

Crop	Maximum biomass yield tonnes (d.w.) ha^{-1} a^{-1}	Source
Higher plants		
Theoretical (C-3 plants) ψ=4.6%	Low 210, mid 170, high 140	(Zhu et al. 2008)
Theoretical (C-4 plants) ψ=6.0%	Low 270, mid 220, high 190	(Zhu et al. 2008)
Sugar cane	74-95	(Klass 1998; Macedo et al. 2008)
Switchgrass	8-20	(Dismukes et al. 2008; Klass 1998)
Corn (grain)	8-34	(Fischer 2002)
Poplar wood chips	11	(Kheshgi et al. 2000)
Soya	4.6-5.5	(Fischer 2002)
Oil palm	8.7	(Fischer 2002)
Microalgae		
Theoretical ψ=12%	Low 410, mid 330, high 280	(Williams and Laurens 2010)
Projected raceway, unspecified algae	110-220	(Huntley and Redalje 2007)
Bioreator raceway, unspecified algae	175	(Chisti 2007)
Best case raceway, unspecified algae	120-153	(Weyer et al. 2010)
Achieved bioreactor (*Phaeodactylum*)	182	(Fernandez et al. 1998)
Achieved raceway (*Pleurochrysis*) over 10 months	60	(Moheimani and Borowitzka 2006)

The dominance of diatoms in marine environment is a result of their unique characteristics: First, diatoms have a low quota for essential trace metals, such as Fe, Mn, Zn, Cu, Co, and Cd (Ho and Subba Rao 2006). Second, diatoms seem to possess a unique carbon fixation (C-4 type) mechanism (Reinfelder et al. 2004) that is much faster than C-3 carbon fixation in other marine algae types (Falkowski and Knoll 2007). The central vacuole in diatoms can absorb and store nutrients efficiently at a sudden trophic increase, exceeding their immediate needs (Tozzi et al. 2004). This is probably a reason diatoms are responsible for most marine blooms. Silica wall (frustule) is the signature feature of diatoms, and it serves as an advantage over other algae types as well. The silica wall serves as a highly effective defense against pathogens such as bacteria and viruses. Once infected, the diatom cell sinks because of the silica wall, thus increasing the chances of survival of the remainder of the community (Falkowski and Knoll 2007). Those features can also serve as advantages while in mass cultivation as diatoms are more viable under harsh conditions, making them ideal candidate as feedstock for biofuel production via hydrothermal liquefaction.

Chapter 2

Literature Review

2.1. Hydrothermal Liquefaction

Hydrothermal liquefaction (HTL) usually takes place at sub-critical condition where the range of temperature for HTL is typically from 200 °C to 400 °C, and pressure from 4 MPa to 20 MPa (Peterson et al. 2008; Karagöz et al. 2006). The region for hydrothermal liquefaction is roughly covered by the blue in Figure 2.1. Such temperature and pressure are close to the conditions for organic matter alteration and further formation into petroleum-like chemicals, which are roughly at >350 °C, and > 15 MPa (Simoneit 1993). Thus, HTL is considered as a mimic of the natural process of petroleum formation.

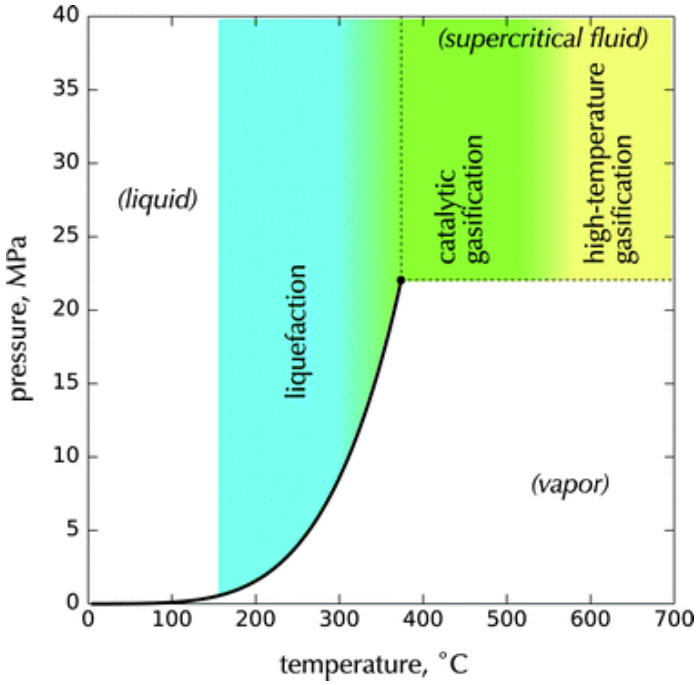

Figure 2.1 Pressure-Temperature phase diagram of water (Peterson et al. 2008)

Under sub-critical conditions, water still remains at liquid phase, but the physical and chemical properties have changed drastically compared to those of ambient water. In general, (sub)-critical water serves as both a better solvent and as a better reactant. Some of the property changes are shown in Figure 2.2.

The dielectric constant (ε_r) of water reflects its polarity: the lower dielectric constant means lower polarity. With the temperature increases, the dielectric constant of water decreases, which results in a better solubility of biological macromolecules (e.g. protein and carbohydrates). Thus a higher temperature is favorable to dissolve the biomass components. The numbers of protons can be reflected by the ionic product (K_w) of water: the higher ion product, the more protons there are. As the temperature increases, the ion product gets higher, which means there are more protons. With more protons in the medium, acid catalyzed reactions are enhanced (Bandura and Lvov 2006). Thus a higher temperature is also favorable as it helps break down the biomass.

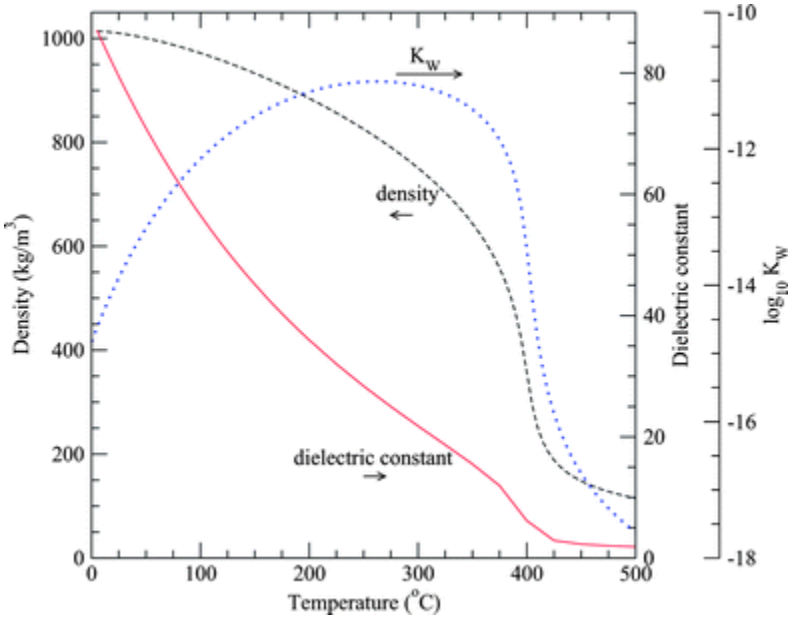

Figure 2.2 Density, static dielectric constant, and ionic product of water at 30 MPa as a function of temperature (Peterson et al. 2008)

2.2. Application of HTL

With such advantages that have been introduced in last section, (sub)-critical used a very important medium in research of biofuel production via biomass and bio-waste. Many kinds of biomass have been studied in hydrothermal liquefaction. They can be roughly categorized as lignocellulosic biomass, algae, and bio waste. Undoubtedly, with different components in the biomass, the products after HTL process are also diverse.

2.2.1. Lignocellulosic Biomass

Chemical Composition

Cellulose, hemicellulose, and lignin are some of the most important structural components of higher plants such as grasses and trees. The sum of these three components in most used lignocellulosic biomass, such as wood residues, corn stalks, and switch grass, is typically more than 90%, with 35-50% cellulose, 20-35% hemicellulose, and 10-25% lignin (Huber et al. 2006; Sun and Cheng 2002; Zhou et al. 2011). Cellulose and hemicellulose are polymers essentially built from sugar monomers, while lignin is an aromatic polymer formed in a much more complicated way with phenylpropanoid as precursor (Pérez et al. 2002). Cellulose is a linear crystalline homopolymer with repeat unit of cellobiose, and is stabilized by the inter- and intra-molecular hydrogen bonding to form strong microfibrils. The microfibrils are bundled by hemicelluloses, amorphous polymers of different sugars to form macrofibrils, and coated with lignin. Among the three compounds, hemicellulose is the most degradable, whereas cellulose and lignin are much more difficult to break down (Taherzadeh and Karimi 2008).

Lignocellulosic biomass has generally been used in biofuel production via two types of hydrothermal liquefaction: direct liquefaction and pretreatment for lignocellulose-to-ethanol production. The degree of decomposition of lignocellulosic biomass is different in each of these two types of processes because of the specific target purposes. Lignocellulose-to-ethanol pretreatment is milder in reaction conditions and shorter in retention time. It aims at decreasing the crystallinity and polymerization of lignocellulosic biomass and improving further enzymatic treatment by increasing the surface area and pore sizes (Zeng et al. 2007). Direct liquefaction aims to completely break down the lignocellulosic biomass into small molecules that potentially can be used as fuel.

General Reaction Mechanism for Lignocellulosic Biomass

As noted above, cellulose, hemi-cellulose, and lignin have different chemical and physical structures. This difference results in different products distribution following hydrothermal liquefaction. Though hemicellulose begins to decompose at relatively lower temperature (Tjeerdsma and Militz 2005), lignocellulosic biomass conversion takes place at higher temperature from 300-330°C better (Akhtar and Amin 2011). Yang et al. (2007) have undertaken extended research on thermal responses of cellulose, hemicellulose, and lignin by thermogravimetric analysis (TGA). The results (Figure 2.3) reveal the behavior of these three polymers in response to heat. Hemicellulose is the first to degrade at 220-315°C, as expected, with its highest weight loss rate occurring at 268°C. Even so, there is still about 25% wt. biomass left as un-decomposable residue. Cellulose begins to decompose rapidly at 315-400°C, with highest weight loss rate at 355°C, and it almost completely decomposes. Lignin has proven to be the most stable compound against heat

among the three and leaves the most (~46% wt.) residue. Under the temperature range for a typical HTL test (200-400°C), it is sufficient to decompose about 70% of hemicellulose and almost all cellulose, but only 30% of lignin.

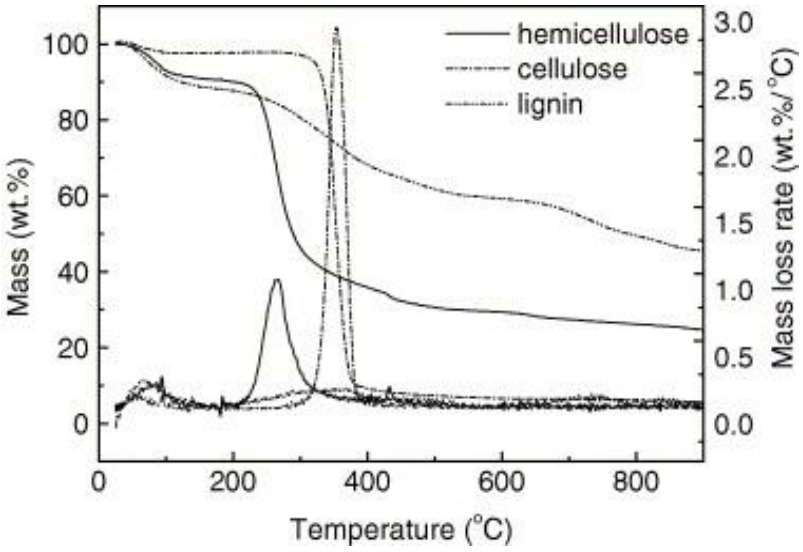

Figure 2.3 TGA diagram of cellulose, hemicellulose, and lignin (Yang et al. 2007)

Different components yield different product as well. The major components in lignocellulosic derived biofuels that are identified by GC/MS are grouped as phenolic compounds, organic acids, oxygen containing heterocyclic rings, and some amount of aldehydes/ketones. Organic acids and oxygen-containing heterocyclic rings (e.g., furfurals) are possibly from cellulose and hemicellulose, while phenolic compounds are more likely from lignin. A simplified reaction mechanism route of hydrothermal liquefaction and/or gasification of cellulose that has been acknowledged widely is shown as in Figure 2.4 (Kruse et al. 2005).

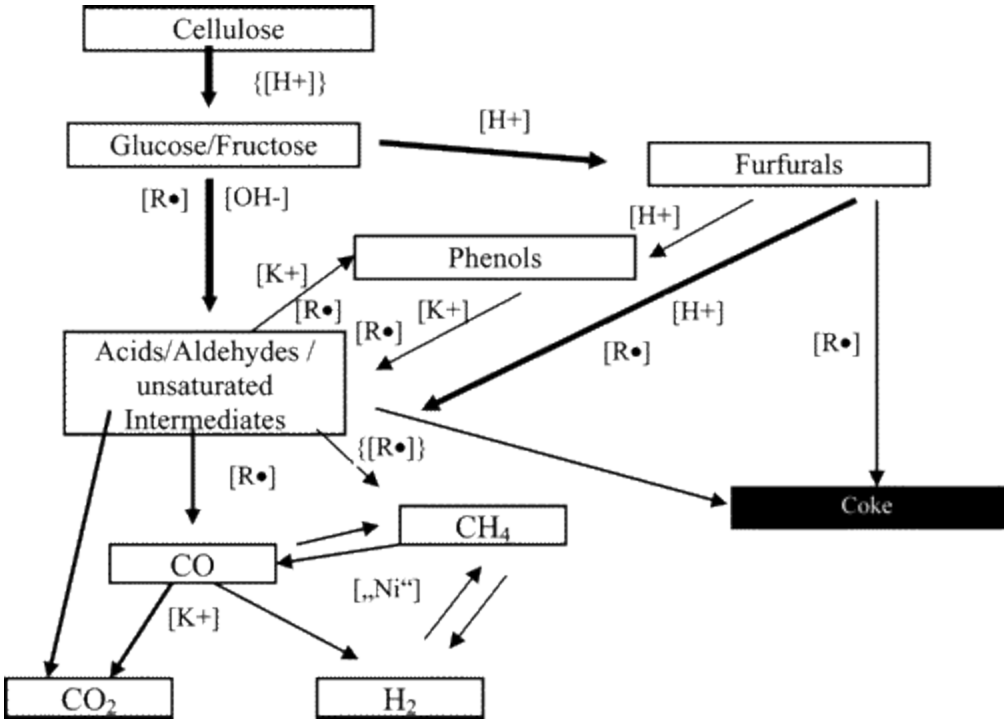

Figure 2.4 Simplified reaction mechanism scheme for hydrothermal liquefaction/gasification of cellulose (Kruse et al. 2005)

Catalysts—in most cases (bi)carbonates, hydroxides of alkali metals—are also used in some studies in both direct liquefaction and lignocellulose-to-ethanol pretreatment, to aim at enhancing the oil quality either through changing the product distribution or reducing oxygen content in some cases (Tekin et al. 2013; Zhou et al. 2011; Karagöz et al. 2005; Karagöz et al. 2006; Lu et al. 2009; Kawamoto et al. 2007; De Bari et al. 2007; Liu et al. 2006).

Table 2.1 Table 2 1 Selected literature of utilization of hydrothermal liquefaction for bioethanol and pretreatment

Feedstock	Temp (°C)	RT (min)	Process Gas	Catalyst	Reactor Type	Main Conclusion	Reference
Direct liquefaction							
Corn stover and *populus tremuloides*	350	10	Nitrogen	n.a.	Batch autoclave	Higher yield with faster heating	(Zhang et al. 2008)
Cherry and cypress	280	15	Nitrogen	K_2CO_3	Batch autoclave	More acetic acid in (hemi)cellulose rich cherry; More phenolics derivatives in lignin rich cypress	(Taherzadeh and Karimi 2008)
Beech and Scots pine	165 - 195	10 - 60	n.a.	n.a.	Batch autoclave	Approx. all acetyl groups of hemicellulose are cleaved at 185°C	(Tjeerdsma and Militz 2005)
Pine sawdust	280	15	Nitrogen	CsOH, RbOH	Batch autoclave	Catalysts increases oil yield and lower char formation.	(Karagöz et al. 2005)
Lignocellulose-to-ethanol pretreatment							
Wheat straw	195	6 - 12	n.a.	n.a.	continuous	70% hemicellulose, 93-94% cellulose recovered	(Petersen et al. 2009)

n.a. not applicable

2.2.2. Microalgae

Chemical Composition

Proteins, carbohydrates, fatty acids (lipids or oils), and inorganics (mainly silica) are of the primary chemical compounds found in microalgae. Unlike higher plants, the carbohydrates in microalgae are usually used as storage products instead of structure components (i.e., cellulose and hemicellulose), which makes them more degradable. In most cases, proteins are the primary organic components in microalgae, followed by carbohydrates, and then lipids (Parsons et al. 1961) under normal condition. However, by manipulating the cultivation environment (e.g. nutrient deficiency to induce stress), lipids-rich microalgae can be obtained at the expense of low productivity (Sheehan et al. 1998).

Current biodiesel technology is based on transesterification. This method utilizes only the lipid content from microalgae or other fatty acid rich crops, but the rest of the biomass is wasted. Even though some research shows the potential for some microalgae species to grow up to 70% of lipids (Chisti 2007), the actual productivity for those specific microalgae is not provided. On the other hand, drying (or harvesting) and extracting microalgal biomass may consume a considerable amount of energy (Lardon et al. 2009) that may compromise the energy recovered from biodiesel. Thus, a better approach is simply to utilize the biomass as efficiently and directly as possible.

General Reaction Mechanism for Microalgal Biomass

Microalgal biofuel via HTL is converted not only from the lipid content, but also from the non-lipid contents, as well, such as proteins and carbohydrates (Dote et al. 1994;

Peterson et al. 2008). However, when multiple kinds of components are involved in the reaction, the mechanism becomes even more complicated.

Protein is a kind of macromolecule that is built up by amino acids through peptide bond. Main reactions such as decarboxylation to amine and deamination to organic acids take place in both amino acids and proteins (Sato et al. 2004; Klingler et al. 2007). Oligomerization of amino acids under hydrothermal conditions is also observed under special experimental setups (Ogata et al. 2000). Sato et al. (2004) conducted a series of experiments to examine the behaviors of five amino acids (30mmol/L): alanine, leucine, phenylalanine, serine, and aspartic acids under hydrothermal condition covering a temperature range of 200-340°C, and fixed pressure of 20MPa. The decomposition of those amino acids were able to described as first-order reaction, although the reaction rates for individual amino acids were different, following the decreasing order of aspartic acid, serine, phenylalanine, leucine, and alanine. A general mechanism of amino acids decomposition was proposed as shown in Figure 2.5. This result was also confirmed by Klingler et al. (2007) using alanine and glycine (0.1% g/g). Temporal wise, with longer residence time, more ammonia was generated, as well as more organic acids, due to deamination. The degradation was quite rapid, as within 20-30s, over 70% of studied amino acids were degraded under 350°C. However, there was no indication of macromolecule formation in either of the studies cited above. One reason for this might be that the concentration of amino acids was too low. Dote et al. (1998) found solid residue after hydrothermal liquefaction of 19 kinds of amino acids of much higher concentrations (4g/100g H_2O). Even though, the oil production was fairly poor as most of the products were water soluble organic compounds other than oil.

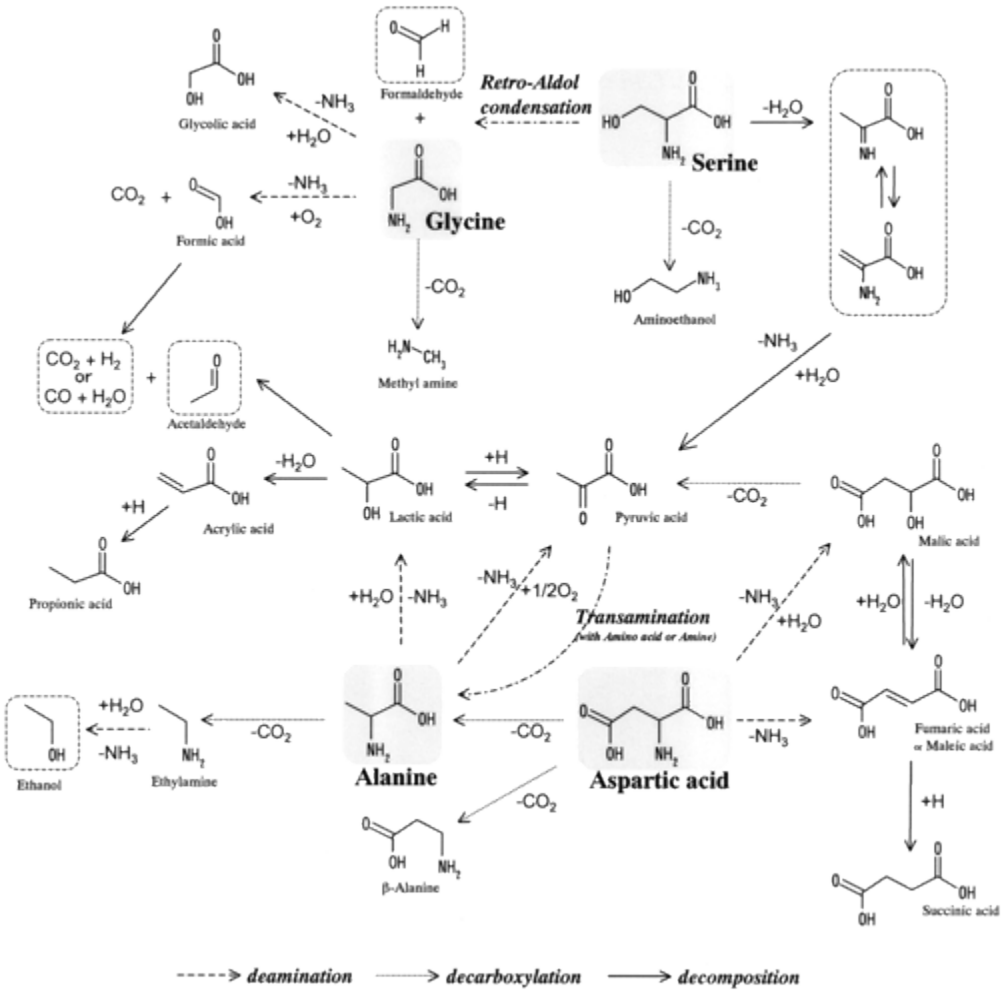

Figure 2.5 Proposed reaction pathways for five selected amino acids under hydrothermal condition. Adopted from (Sato et al. 2004)

Though proteins can be hydrolyzed into amino acids, this process is not fast enough to release all the building blocks in a short time, and thus we may expect proteins to behave differently under hydrothermal conditions. In earlier research on hydrothermal liquefaction of protein (albumin from egg) rather than of amino acids, Dote et al. (1996) discovered that oil yield was quite low under a temperature of 200°C. One conclusion that they drew from the results was that albumin decomposed to ammonia, not amino

acids, through hydrolysis. Wang's doctoral dissertation (Wang 2011) illustrates that fatty acids and their derivatives such as n-hexadecanoic acids, N,N-dimethyl-hexadecanamide, N-methyl-hexadecanamide, Octadec-9-enoic acid, dodecanamide, N,N-dimethyl-9-octadecenamide, and [Z]-9-octadecenamide were found under temperatures higher than 260°C by using only egg albumin. The formation of fatty acids from pure protein feedstock is quite intriguing that it makes it possible to produce oil (fatty acids) from only protein-containing biomass. The yields of protein to crude oil were not very high from Dote's and Wang's research: about 10% (300°C) and 20% (300°C) respectively.

Proteins are also able to react with aldose sugar under hydrothermal condition in a mechanism called Maillard reaction (shown in Figure 2.6) to stabilize the free radical generated in heat (Kruse et al. 2005). Because of this alternative pathway, the product distribution of microalgal biofuel via hydrothermal liquefaction is much different from that of lignocellulosic biomass: fewer phenols and aldehydes, less gas yield, but more nitrogen-containing cyclic compounds (Kruse et al. 2007).

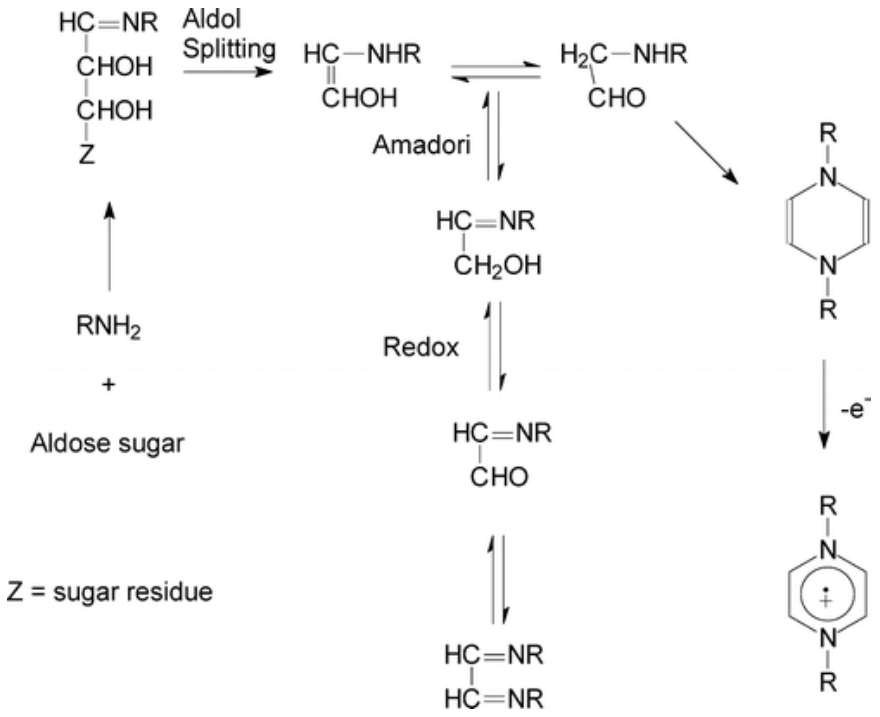

Figure 2.6 Scheme for Maillard reaction (Kruse et al. 2007)

Lipids are other major components in microalgal biomass, as well as the most desired components for biofuel yield. Triacylglycerols (TAGs) are a group of lipids that can serve as storage substances and energy sources under difficult conditions. TAGs are the preferred lipids that should be distinct from other lipids, such as phospholipids, because of their membrane structure, etc. TAGs can be hydrolyzed under hydrothermal condition, releasing three long chain fatty acids and one glycerol. Glycerol is water soluble and is easier to convert into other water soluble compounds under hydrothermal condition, thus it is in most cases kept in the aqueous phase before and after reaction. Fatty acids are generally more stable under hydrothermal condition. Holliday et al. (1997) achieved >97% recovery of 4 types of triglycerides to fatty acids under hydrothermal condition. Hydrolysis could be completed at 270-280°C with 15-20min, but it was very

sensitive to temperature. To reach the same hydrolysis degree for linseed oil at 260°C and 280°C, it took 69 min and 20 min respectively.

Fatty acids can be further "upgraded" into long chain hydrocarbons via catalytic reactions. Watanabe et al. (2006) tested the decarboxylation of several homogeneous and heterogeneous catalysts on stearic acid (17C-acid). Stearic acid is fairly stable in hydrothermal condition, with only 2% conversion at 400°C, 30 min. However, with homogeneous catalysts, namely NaOH and KOH, the conversion is increased to 13% and 32% respectively, and the main products are 17-carbon alkane and CO_2. Heterogeneous catalysts delivered a much higher conversion rate: CeO_2, Y_2O_3, and ZrO_2 enhanced the conversion of steric acid to 30%, 62%, and 68% respectively, and the main products were 16-carbon alkene and CO_2. Another study conducted by Fu et al. (2011) using two kinds of activated carbons showed the decarboxylation effect on palmitic acid (15C-acid) and oleic acid (17C-acid, monounsaturated) under 370°C, 3 hrs. Direct decarboxylation reaction was observed. However, tests with oleic acid showed a high yield of stearic acid, which is the saturated comparative of oleic acid. With no addition of hydrogen, the author suggested that the extra hydrogen atoms might come from another oleic acid molecule or solvent (water) via water-gas-shift reaction.

Microalgal biomass can be treated as a complexity of the major groups mentioned above. The reaction mechanism for each individual group is yet undiscovered fully, thus the interaction between the groups is even more obscure. When microalgae are used as feedstock in hydrothermal liquefaction, the yield of bio crude oil varies from species to species, because of different chemical component ratios, reaction conditions (e.g., temperature and retention time), as well as catalysts. Table 2.2 selects representative

literature, which shows the various yields of *Spirulina*. From this table we find that the highest reported yield is more than 4 times higher than the lowest, even though the experimental conditions were similar. Most studies have presented very close product spectra by GC-MS analysis, yet a few report very different product distributions. All these differences between individual research results indicate that hydrothermal liquefaction of microalgae is a very complicated process.

Table 2.2 Selected literature of *Spirulina* biofuel production via hydrothermal liquefaction

Feedstock	Lipid content (% d.w.)	Temp (°C)	Retention time (min)	Catalyst	Yield (% d.w.)	Typical products/ Remarks	Reference
Direct liquefaction							
Chlorella valgaris/ *Spirulina* sp.	n.a.	300/350	60	1M Na_2CO_3 KOH CH_3COOH HCOOH	C: 19.1-27.3; S:11.6-20,	Mono-aromatics, substituted phenols, N heterocycles, long chain acyls	(Ross et al. 2010)
Spirulina platensis	11.2%	200-380	0-120	n.a.	17-39.9	39.9% optimal at 350C, 60min, 20% solid; Different grouping method but similar compounds as in previous entry	(Jena et al. 2011)
Spirulina platensis	11.10 ±1.52	300-350	30-60	5% wt Na_2CO_3 NiO $Ca_3(PO_4)_2$	30.2(NiO) 34.5 ($Ca_3(PO_4)_2$) 39.9(none) 51.6 (Na_2CO_3)	more monoaromatics were found with Na_2CO_3 and NiO, less aliphatics and polyaromatics	(Jena et al. 2012)
Spirulina sp.	5	300	30	n.a.	32.6	High nitrogenous compounds yield, no straight chain hydrocarbons were identified	(Vardon et al. 2011)

n.a. not applicable

Chapter 3

Materials and Methods

3.1. Feedstock

The diatoms used in this study were obtained from Jawkai Bioengineering R&D Center, Ltd. (Shenzhen, China). The products were mainly *Skeletonema costatum*, but a few other species such as *Nitzschia* spp. and *Chaetoceros* spp. were also identified by microscope. Diatoms were harvested by centrifuge (16K rpm), dried at temperature less than 100 ℃, ground into fine powder, and then sieved for particles larger than 300 μm.

Moisture content was measured as the weight loss in 105 ℃ oven until the weight was constant. Ash content was measured as the residue in 600 ℃ furnace until the weight was constant. General properties, chemical composition, and partial elemental composition were tested by Midwest Lab (Omaha, NE). Crude protein was measured by Kjeldahl method and crude fat by Soxhlet extraction. Other properties were analyzed by the methods suggested by Association of Official Analytical Chemists (AOAC). CHN and Silicone composition were tested by Microanalysis Lab at the University of Illinois (Urbana, IL) using CHN analyzer (CE-440, Exeter Analytical Inc., MA), and ICP-OES (Optima 2000DV, PerkinElmer Inc., MA), respectively . A summary of characteristics of diatoms feedstock is concluded in Table 3.1.

Table 3.1 Characteristics of diatom feedstock

Properties	Diatom feedstock (%)	*Sk. costatum* (Parsons et al. 1961) (%)	*Sp. platensis*
General Properties			
Moisture Content [a]	11.45	n.a.	6.5
Ash Content	32.8	39	9.5
Chemical Composition			
Crude Protein	38.7	37	64.4
Crude Fat	3.70	4.7	5.1
Acid Detergent Fiber	17.2	Reported as total	0.7
Neutral Detergent Fiber	21.0	carbohydrate	2.1
		20.8	
Lignin	6.53	n.a.	0.2
Elemental Composition			
C	31.9	31.3	49.3
H	4.26	4.4	6.4
N	5.96	n.a.	11.0
Si	6.76	14.3	n.a.
Miscellaneous [b]	9.02	n.a.	n.a.
O [c]	42.1	n.a.	33.3

All data calculated based on dry weight except noted otherwise.
a: calculated as received. b: sum of S, P, Mg, Ca, and Na. c: calculated by difference

3.2. Hydrothermal Liquefaction (HTL) Process

100mL batch reactors (Model 4593, Parr Instrument Co., Moline, IL) were used to conduct the HTL experiments. Samples were adjusted to 30% solid weight (w/w) by mixing tap water and diatom powder. Each reactor vessel was loaded with 70g diatom paste. Headspace was purged by pure nitrogen for three times, and then sealed with 90 psi initial pressure. Magnetic drive was used to mix the feedstock at 300 rpm during the reaction. The reactor was heated by an electric resistance heater to desired temperatures, held for a period of time which was defined as retention time, and finally cooled down

rapidly by running tap water through the cooling coil. Reaction temperature was set at 260°C, 280°C, 300°C, and 320°C; Reaction time was set at 30min, 45min, 60min, 75min, and 90min for each temperature.

A typical heating curving is as shown in Figure 3.1. The heating period was 40-60 minutes long, depending on the designated final temperature. The heating rate was faster from 0 to 200°C at approximately 9.38°C/min, and then it slowed down to about 3°C/min until it reached the designated temperature. The variation of temperature during retention time is within 3°C. Cooling was achieved by running tap water through the cooling coil at about 9.11°C/min. Pressure was built up stably, and then remained stable during retention time.

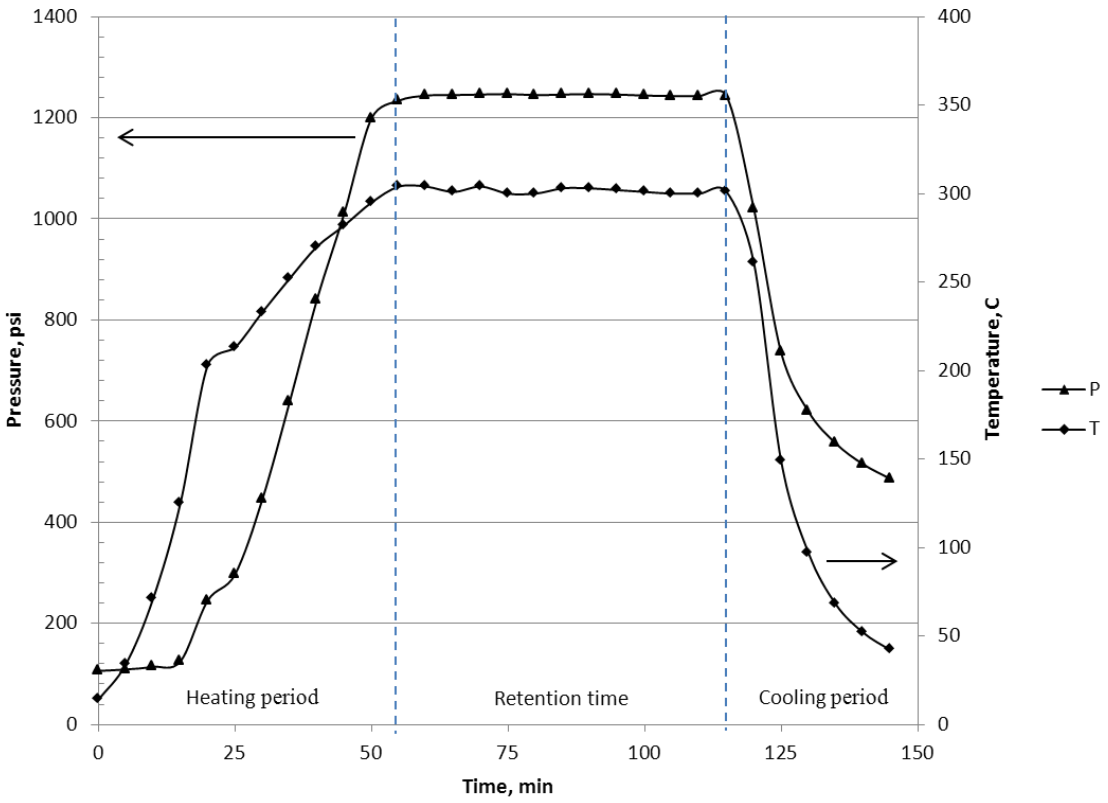

Figure 3.1 Temperature and pressure profile of a typical HTL test at 300°C with 1 hour retention time

Pressure was naturally built. However, about 90 psi nitrogen was applied at the beginning of reaction. The initial pressure was to make sure that water would remain in liquid phase throughout hydrothermal liquefaction process. As we can see from the pressure profile, it always remained above boiling pressure, which prevented excessive water vaporization.

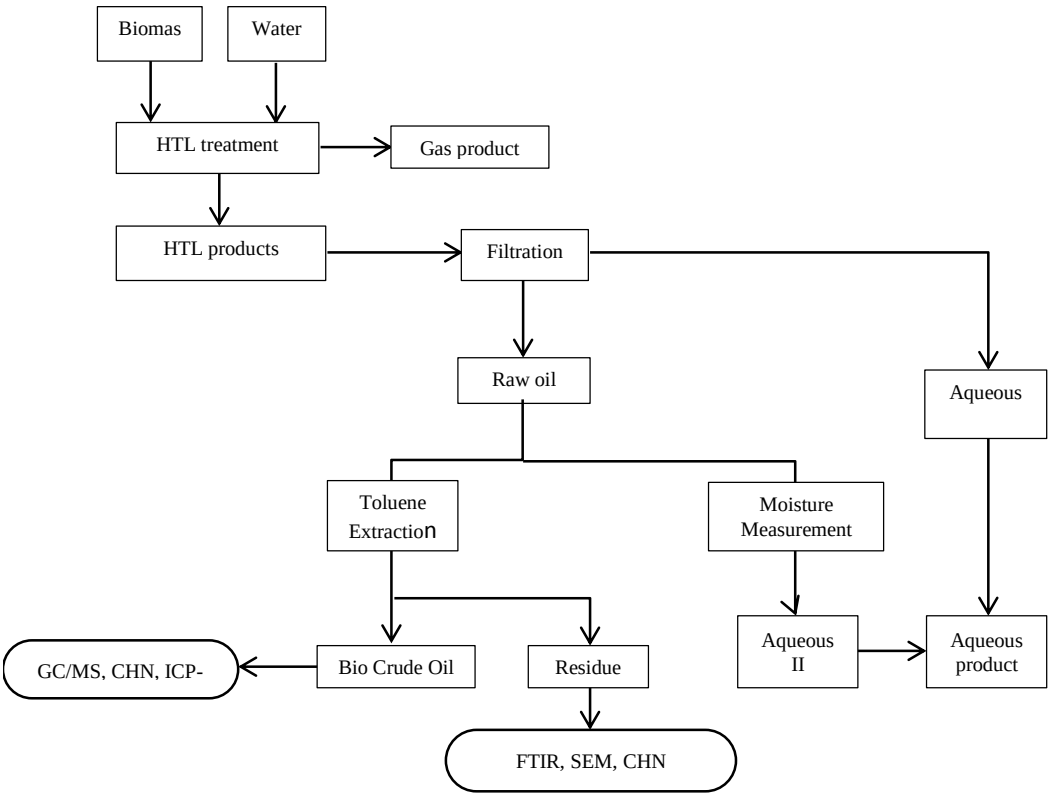

Figure 3.2 Product recovery procedure

The product recovery procedures are shown as Figure 3.2. Only liquid and solid products were carefully collected for future analysis, and the gas product was released after cooling was completed. The yield of gas product was calculated according to ideal gas law using residual gas pressure and estimated gas molecular weight (44, as CO_2

shared >90% of gas component according to previous studies in our group) (Anastasakis and Ross 2011; Biller and Ross 2011). The collected products were vacuum filtered (Whatman #42 ashless filters) to separate the liquid and solid products. The solid product is defined as raw oil. The raw oil contains a part of aqueous product, bio crude oil, and solid residue (ash content and formed char). Bio crude oil was defined as the toluene soluble fraction in the raw oil after HTL process, whereas the solid residue is the toluene insoluble fraction. Bio crude oil and solid residue were separated by Soxhlet extraction method as described in ASTM Standards D473-02 and D4072-98. The moisture content of the raw oil was determined according to ASTM Standard D95-99. Approximately 3g raw oil was used in 100mL solvent for both moisture content tests and Soxhlet extraction.

Product yields are defined as below (Table 3.2):

Table 3.2 Hydrothermal liquefaction products measurement and calculation

Measurement (g)	**Symbol**
Mass of diatom feedstock	M_f
Mass of diatom feedstock dry mass	$M_{f.d}$
(Estimated) Mass of gas product	M_g
Mass of raw oil	M_{raw}
Mass of solid residue	M_{res}
Mass of water in raw oil	M_w
Product	**Equation**
Gas yield (%)	$= \frac{M_g}{M_{f,d}} \times 100$
Raw oil yield (%)	$= \frac{M_{raw} - M_w}{M_{f,d}} \times 100$
Bio crude oil yield (%)	$= \frac{M_{raw} - M_{res} - M_w}{M_{f,d}} \times 100$
Solid residue yield (%)	$= \frac{M_{res}}{M_{f,d}} \times 100$
Aqueous product (%)	$= \frac{\left(M_{f,d} - M_g - (M_{raw} - M_w)\right)}{M_{f,d}} \times 100$
Toluene insolubility (%)	$= \frac{M_{res}}{M_{raw} - M_w} \times 100$

3.3. Crude Biofuel Characterization

3.3.1. CHN Composition and Heating Value Estimation by Calorimeter

CHN analysis of solid product and the residue after extraction was conducted to estimate the CHN content in the crude oil. An estimation method based on mass balance is used in this study to determine the CHN composition in bio crude oil. All samples sent to CHN analysis were dried overnight in 105°C oven, thus there was no moisture content

in all samples. CHN analyzer (CE-440, Exeter Analytical Inc., MA) was used by taking approximately 1~3 mg samples. Each sample was duplicated to ensure accuracy.

Because measuring the heating value of bio crude oil in this study was unfeasible due to the limitation of the amount of bio crude oil sample, an estimation method was used instead: Heating value of raw oil was tested by calorimeter (Parr 6200 Calorimeter, Parr Instrument Co., Moline, IL). The estimation of bio crude oil is calculated as the obtained heating value of raw oil divided by the combustible portion. All samples were kept in the oven at 105°C for drying. All samples were pressed into pellets with a diameter of 5mm.

3.3.2. GC/MS Analysis

GC/MS analysis was used to identify the components in the bio crude oil, and by extension, to determine the quality of it. Samples were made from the toluene dissolved bio crude oil from Soxhlet extraction. All samples were prepared with Whatman 0.45μm filter prior to injection. Agilent 6890 GC coupled with Agilent JW Scientific DB-5 GC Column (J&W 123-5032; 30m×0.32mm i.d., 0.25μm film) (Agilent Inc., Palo Alto, CA) was used for separation. 1μL sample was injected at 250°C, with a split ratio of 5:1, and with helium as carrier gas at a flow rate of 4 ml/min. The oven temperature was initially at 50°C and held for 5 min, and then increased to 315°C at a rate of 5°C/min and then held for 5min. Ionization was caused by positive electron impact (EI) at 69.9eV, and scan range was from 35 to 800 m/z.

All spectra were analyzed using HP Chemstation (Agilent, Palo Alto, CA) and AMDIS program (NIST, Gaithersburg, MD). Individual peaks were also compared with

NIST Mass Spectral Database (2008) and W8N08 library (John Wiley & Sons, Inc., USA).

3.3.3. SEM and FT-IR Characterization

Diatoms feedstock, solid residue after toluene extraction, and ash content were analyzed by SEM and FT-IR in order to examine the morphology of the frustules. Products at 320°C reaction temperature and 90 min reaction time were selected as representative samples.

High resolution environmental scanning electron microscope (Philips XL 30 ESEM-FEG) was used to confirm the diatom species and examine the morphology of frustules. Coupled with an EDAX light element energy dispersive spectroscope, this instrument also provided elemental composition on selected surfaces with controllable sizes. All samples were coated with Au/Pd in turbo-pumped sputter coater (Denton Vacuum Desk II TSC) to the thickness of approximately 6 nm.

FT-IR was used as a supplementary interpretation for the samples examined by SEM. Bulk information of functional groups found in the samples could be obtained to help us understand what was going on between the samples chemically. FT-IR instrument used was Thermo-Nicolet Nexus 670 model at 1 cm^{-1} resolution from 800 cm^{-1} - 4000 cm^{-1}. Samples were prepared by mixing and grinding with KBr, with sample to KBr ratio of 1:121, then a proper amount of prepared samples was pressed to 7mm pellets.

Chapter 4

Results and Discussions

The bio crude oil produced from diatoms is not the viscous black fluid obtained from microalgae of lower ash content, but instead, presents itself in solid phase. In other words, it is absorbed on the solid residue. Thus prior to any further analysis, the solid residue with bio crude oil must be carefully ground and well homogenized to ensure consistency.

4.1. Effects of Reaction Temperature and Reaction Time

The products from diatoms after hydrothermal processing were in three different phases: namely, gas phase, aqueous phase, and solid phase. Biofuel was absorbed in the solid phase product, thus extraction was necessary to separate bio crude oil from solid residue. The effects of temperature on the distribution of biofuel products are shown in Figure 4.1. As we can see from this figure, gas fraction and bio crude oil fraction increased as temperature increased, whereas solid residue and aqueous fraction decreased as temperature went up. The increase of gas fraction was a result of gasification, which is favored at higher temperatures, even though temperature of 320°C is not really a typical gasification zone (800°C~1000°C). More bio crude oil and less solid residue were also found. This is probably more biomass was converted into bio crude oil from diatom biomass, and less was converted into char.

The yields of bio crude oil from diatoms were between 12.95% (dry weight, d.w.t.) to 33.37% (d.w.t.). The highest yield was 35.6% (d.w.t.) at 320°C and 75 min. The lowest yield was 12.95% at 260°C and 75 min. Generally, higher temperature and longer

retention time resulted in higher bio crude oil yield in the selected experimental condition range, which agrees with literature. However, as the ash content in the diatom is as high as 39%, if we subtract the ash content and only count in the volatile substance, the yield will be between 21% (volatile weight, v.w.t.) and 59% (v.w.t.), which is very high compared to other species of microalgae, even to some of lipid-rich species with addition of catalysts (Biller and Ross 2011; Brown et al. 2010; Zou et al. 2009; Yang et al. 2004). For the convenience and being practical, all data reported will still be based on total dry mass with ash content counted in.

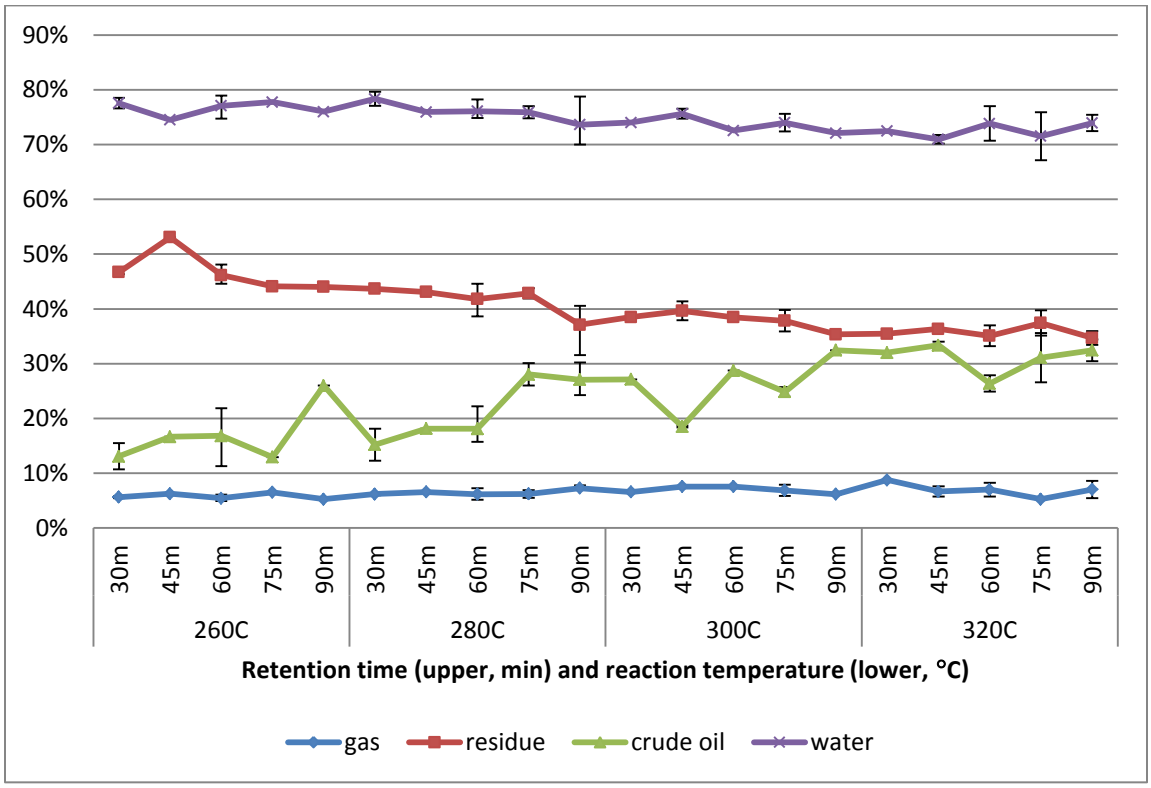

Figure 4.1 Effects reaction temperature and retention time on the products distributions, error bars are the range of the data

Then yield of bio crude oil is generally increasing with higher reaction temperature and longer retention time. This finding is similar to our previous work with regard to the yields from *Spirulina* and *Chlorella*, but the correlation is less significant. This phenomenon might be caused from the different phases of the products between diatoms and the other two microalgae species. The bio crude oil from diatoms is contained in a solid phase because of the high ash content due to frustules; while the bio crude oils from *Spirulina* and *Chlorella* are in viscous liquid phase. The bio crude oil might be absorbed by the porous frustules, instead of being miscible in the subcritical water as those from *Spirulina* and *Chlorella*. This also caused the reaction taking place in liquid-solid phase so that the reaction rate was also limited by the active surface area. As we kept the amount of diatoms consistent, which means the surface area in each reaction was also comparable. Temperature in this case is a factor that could affect the equilibrium between absorption and desorption of the oil on the frustule surface. As we can also see from this figure that in general, higher temperature resulted higher bio crude oil yield. Retention time also had positive correlation to the yield, as the equilibrium tended to be reached over time.

In the products from diatoms, there are some small, thin, white flakes produced, which is absent in that low ash content microalgae. This unique product is believed to be a mixture of crystalized salts from diatom biomass and condensed frustules. Further analyses were also conducted to reveal its composition, which will be discussed in following sections later.

The solid residue generated from diatom hydrothermal liquefaction may limit its application in industry due to the phase separation of bio crude oil from ash content, as

well as its build-up may impede the proceeding of the reaction, or even block the reactor wall if scaled to continuous process.

4.2. CHN Analysis and Higher Heating Value Estimation

CHN compositions of dried raw HTL product and solid residue were analyzed to estimate the CHN composition of bio crude oil. The CHN composition change with regard to temperature and retention time can be seen as below:

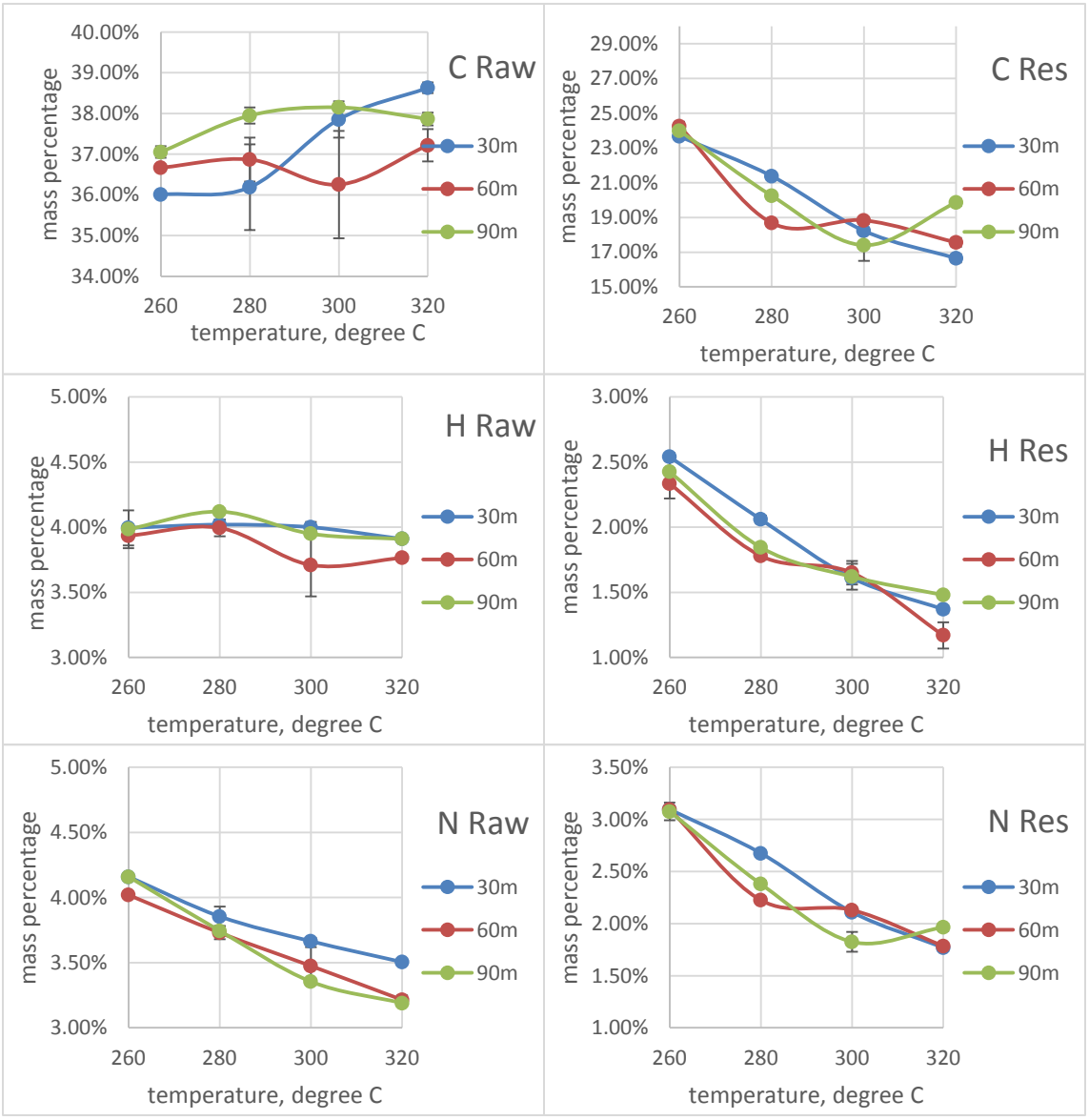

Figure 4.2 CHN elemental composition of HTL raw oil product and solid residue after extraction, error bars are the range of the data

As it is shown in the Figure 4.2, there is an apparent trend of how CHN element changes with respect to different hydrothermal conditions. In the raw products (bio crude oil + residue) of different experimental conditions, the carbon content increased with lower temperature over time. However, the carbon content increasing rate was very significant from 280°C to 320°C in 30min. In fact, under 320°C and 30 min hydrothermal condition, the carbon composition was the highest. Explanation to this result is possibly that the temperature is high enough for diatom biomass to hydrolyze, but the retention time is not enough for it to further assemble to oily compounds. Hydrogen content was kept relatively constant. Nitrogen content, however, decreased substantially as the temperature was raised. This result agrees with other studies regarding to nitrogen distribution in hydrothermal products: higher temperature leads to more severe deamination. The amino group is cleaved and then reform as ammonia, or other small, water soluble molecules and remain in aqueous products (Yu et al. 2011; Dote et al. 1998).

The trends of CHN element changes are more obvious to interpret in solid residue. The carbon content decreased significantly with regard to the increasing temperature. Nevertheless, it showed an inversed trend at the temperature of 320C, where longer retention times caused more carbon left in the residue, or less carbon recovered in bio crude oil, which is because of the formation of char under this temperature.

With CHN concentration in raw oil products and solid residues after extraction, it is possible for us to calculate the CHN content in the crude oil using the following equation:

$$CHN\%(oil) = \frac{CHN\%(total) - CHN\%(res) \times TI}{1 - TI}$$

The CHN values in crude oil are showed in the following Table 4.1. This table shows that C and H contents in most of the crude oils are similar but the N content is less in higher temperature and longer retention time conditions. This is possibly because under those conditions, nitrogen is converted into water soluble compounds and thus the distribution in the crude oil is reduced.

Table 4.1 Estimated bio crude oil CHN composition

	C	H	N		C	H	N		C	H	N
90m				**60m**				**30m**			
320C	49.37%	5.46%	3.97%	320C	49.79%	5.42%	4.13%	320C	52.69%	5.53%	4.61%
300C	51.41%	5.44%	4.33%	300C	47.39%	5.03%	4.33%	300C	50.40%	5.53%	4.66%
280C	49.27%	5.57%	4.62%	280C	48.50%	5.41%	4.69%	280C	45.66%	5.27%	4.61%
260C	45.40%	4.98%	4.85%	260C	44.61%	4.96%	4.61%	260C	43.90%	4.93%	4.84%

Based on dry mass

Heating values of the bio crude oil were provided by calorimeter. Dried raw oil was used for this estimation by deducting the ash content (residue weight in Table 4.2). The heating values of selected samples are listed below as in Table 4.2.

Table 4.2 Estimation of higher heating values of selected bio crude oil samples

Temperature (°C)	retention time (min)	sample weight (g)	Residue weight (g)	HHV (MJ/kg)	Corrected HHV (MJ/Kg)
260	30	0.514	0.194	17.48	28.08
	60	0.525	0.205	17.61	28.90
	90	0.535	0.197	17.13	27.11
280	30	0.525	0.215	17.62	29.84
	60	0.554	0.221	17.84	29.67
	90	0.535	0.207	18.18	29.65
300	30	0.544	0.200	18.86	29.83
	60	0.534	0.206	18.22	29.66
	90	0.525	0.211	18.75	31.34
320	30	0.538	0.206	19.71	31.95
	60	0.526	0.225	18.79	32.83
	90	0.513	0.214	18.78	32.21
feedstock		0.555	0.149	14.62	19.18

Feedstock contains 11.45% moisture content
Ref: HHV of gasoline is 48 MJ/kg

The HHVs of the bio crude oil ranged from 28.08 MJ/kg to 32.83 MJ/kg. The heating value increases with higher temperature and retention time. All bio crude oil samples have much higher heating value compared to that of diatom feedstock, which is only about 19 MJ/kg. This indicates that the energy intensity of the bio crude oil is concentrated. However, compared to the heating value of gasoline, this value is not high enough.

4.3. GC/MS Analysis

There are more than 100 identified chemical compounds from the GC-MS analysis but most of them are of low signals. Most commonly identified compounds with relatively higher abundance in the bio crude oil are shown in Table 4.3.

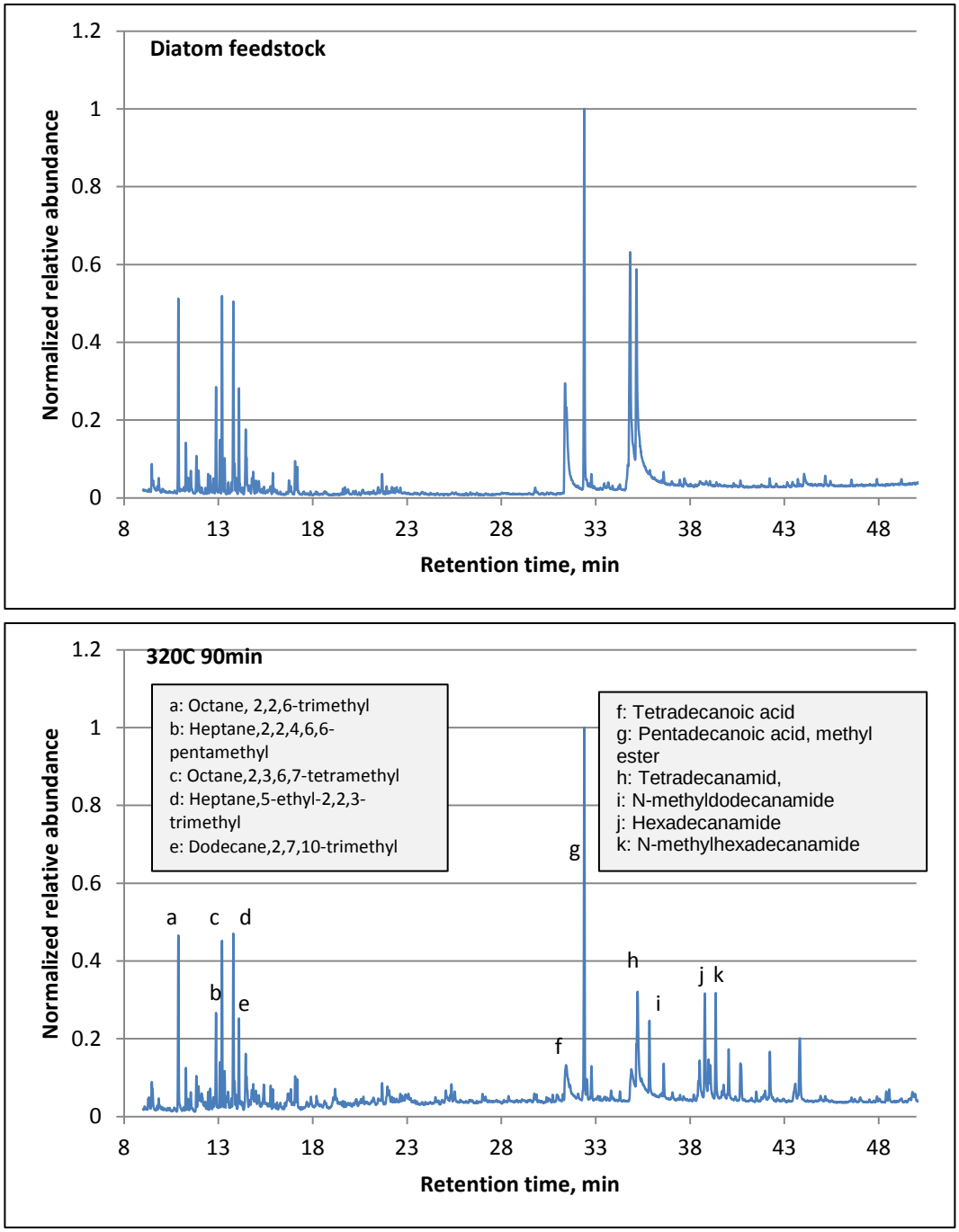

Figure 4.3 GC spectra of toluene extracted untreated diatom feedstock and bio crude oil at 320C 90min and major identified peaks.

Table 4.3 Most commonly identified compounds in the bio crude oil in GC/MS analysis

Identified compounds	Retention time (min)
Heptane, 2,2,4-trimethyl-	8.3661
Octane, 3,3-dimethyl-	8.92
Pyrazine, 2,5-dimethyl-	9.2995
Octane, 2,2,6-trimethyl-	10.8776
Heptane, 2,2,3,5-tetramethyl-	11.2777
Octane, 2,3,3-trimethyl-	11.8334
Pyrazine, 2-ethyl-6-methyl-	12.0487
Heptane, 2,2,4,6,6-pentamethyl-	12.8755
Octane, 2,3,6,7-tetramethyl-	13.1935
Decane, 2,6,8-trimethyl-	13.3311
2-Pyrrolidinone, 1-methyl-	13.4054
Heptane, 5-ethyl-2,2,3-trimethyl-	13.7936
Dodecane, 2,7,10-trimethyl-	14.0894
Pentane, 3,3-dimethyl-	14.4501
1-Ethyl-2-pyrrolidinone	15.3904
Sulfurous acid, 2-ethylhexyl nonyl ester	17.0694
Tetradecanoic acid	31.4294
Pentadecanoic acid, methyl ester*	32.398
Hexadecenoic acid, Z-11-	34.907
n-Hexadecanoic acid	35.1558
Tetradecanamide	35.225
N-Methyldodecanamide	35.8491
N,N-Dimethyldodecanamide	36.6065
9-Octadecenamide, (Z)-	38.5077
Hexadecanamide	38.7847
N-Methylhexadecanamide	39.36
N, N-Dimetylpalmitamide	40.049
N-Decanoylmorpholine	43.8224

*internal standard

All the identified compounds can be categorized into the following groups: alkanes, fatty acids and their derivatives, benzenes, nitrogen-containing hetero-aromatics, and other oxygen-containing compounds (usually with several oxygen atoms). Those chemical groups are usually found in bio crude oil from other microalgae species as well. Alkanes, N-containing hetero-aromatics, and benzenes are smaller molecules that have a shorter retention time in GC which is usually less than 20 minutes; while on the other hand, fatty acids and their derivatives are much heavier and usually are to be found after 30 minutes retention time. In Figure 4.3, the alkanes regions of the GC spectra from different untreated and treated biomass turned out to be very similar, except for the relative abundance. The fatty acyls region differed somehow as there were more compounds found. As there are no free short-chain alkanes in the diatom biomass originally, it is assumed that the alkanes were possibly generated during the heating period and maybe during Soxhlet extraction, and frustules might have played an important role in the conversion.

Figure 4.4 shows the trend of the distribution of these groups of chemicals in the bio crude oil regarding to (a) different reaction temperatures at the same reaction time (90min), and (b) different reaction times at the same reaction temperature (320°C). These two diagrams were generated with the relative peak area of identified compounds, and the comparison between two conditions does not necessarily reflect the absolute amount of relative compounds due to lack of standard/working curve. Even though there is some inconsistency especially regarding to the amount of alkanes in the bio crude oil at all conditions, there are some vague trend in the compounds distribution under different conditions. As we can see from the figures that N-containing hetero-aromatic content has

a negative correlation with regard to the temperature and retention time. That is, the amount of N-containing hetero-aromatics tends to be less with higher temperature and longer retention time. Such result is consistent with the literature in nitrogen distribution studies that more amino groups were cut off from amino acids prior to folding and polymerization for bio crude oil (Yu et al. 2011; Dote et al. 1998). Fatty acids and their derivatives did not change too much as we expected in higher temperature. This result might have shown that 320°C is not sufficient to induce thermal cracking of fatty acids. However, this result may suggest that it is not needed to get to very high temperature and long retention time to get the same quality of bio crude oil, and these two factors are better to be determined just by the yield of bio crude oil.

Interestingly, as there is only about 3.7% d.w.t. crude fat in diatom feedstock, the amount of fatty acids shares almost the half of the peak area of identified compounds. The GC-MS analysis of diatom feedstock extract and bio crude oil also suggested that there was a substantial improvement of fatty acids/derivatives in the bio crude oil. However, how much amount of fatty acids/derivatives was formed from protein is still unknown due to lack of quantitative data. The increase of fatty acids/derivatives is most likely formed from protein in the biomass. Hexadecanamide ($C_{15}H_{31}CONH_2$) and N-methylhexadecanamide ($C_{15}H_{31}CONH(CH_3)$) were newly found abundant fatty acid derivatives in the crude oil, which is absent from the feedstock. However, the exact mechanism of how protein is converted into fatty acids is absent from the literature and it is difficult to propose one due to the complexity of the biomass in this study.

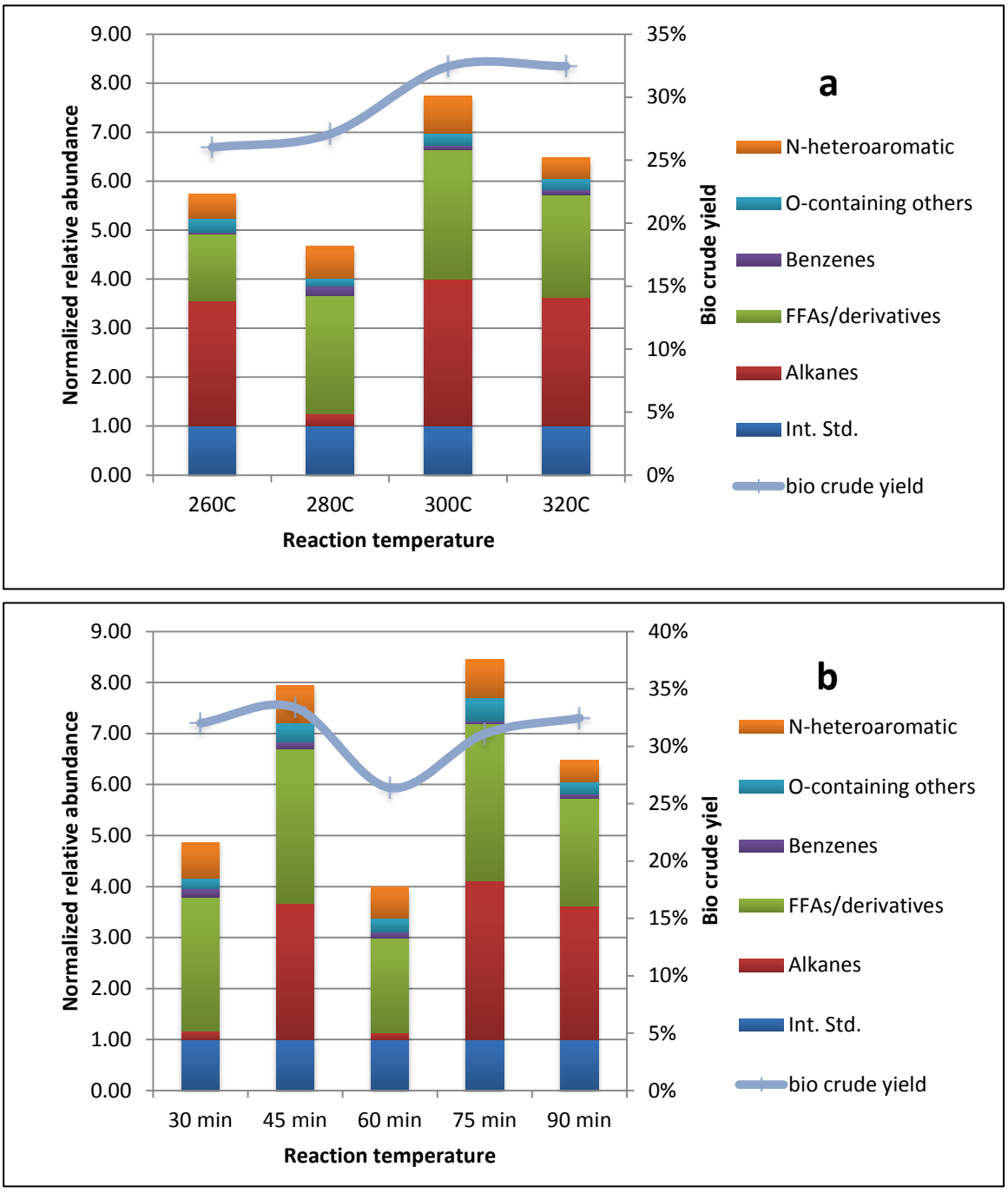

Figure 4.4 Normalized peak areas of different categories of identified chemicals influenced by a) reaction temperature under the same retention time (90 min), b) retention time under the same reaction temperature (320C). Normalized by internal standard C15 fatty acid methyl ester of 0.5 umol.

There is a huge difference in identified hydrothermal liquefied products between diatoms and other microalgae species. For example, in Duan et al.'s study (Duan and Savage 2010) with *Nanochloropsis sp.* they found a great amount of alkane and fatty acids. However, the most abundant fatty acids in this study were palmitic acid ($C_{15}H_{31}COOH$), which is one carbon more comparing to that in diatom bio crude oil. There were many monoaromatics (i.e. benzene and its derivatives) that shared up to 20% of total peak area found in hydrothermal liquefaction of *S. platensis* with no added catalysts in Jena *et al.*'s study (Jena et al. 2012; Jena et al. 2011). However, we did not find as much amount of monoaromatics in bio crude oil from diatoms. Yu (Yu 2012) found in his research with *Sp. plantensis* that the N-containing hetero-aromatic compounds tended to increase with the increase of reaction temperature, and they were of >30% of the total identified peak area. However, in this research with diatoms, we found that this group of compounds was only about 10% of the total identified peak area, or less. This group of compounds may be viewed as undesirable products as they are chemically stable because of the presence of nitrogen and the aromatic structure. Besides, they may be hazardous to metal catalysts when further upgrading of bio crude oil is desired because the affinity of nitrogen atom to noble metal catalysts.

One preliminary test of *Sp. plantensis* and diatomaceous earth (frustules) mixture under the condition of 300°C and 60 min showed increase of hexadecane-framed alkanes (Figure 4.5), and decrease of hexadecanamide. This discovery might have suggested that the addition of frustules did help with decarboxylation of fatty acyls to generate more alkane components. However, to draw a firm conclusion about the effect of frustules calls more comprehensive and careful experiments, which is proposed as future research.

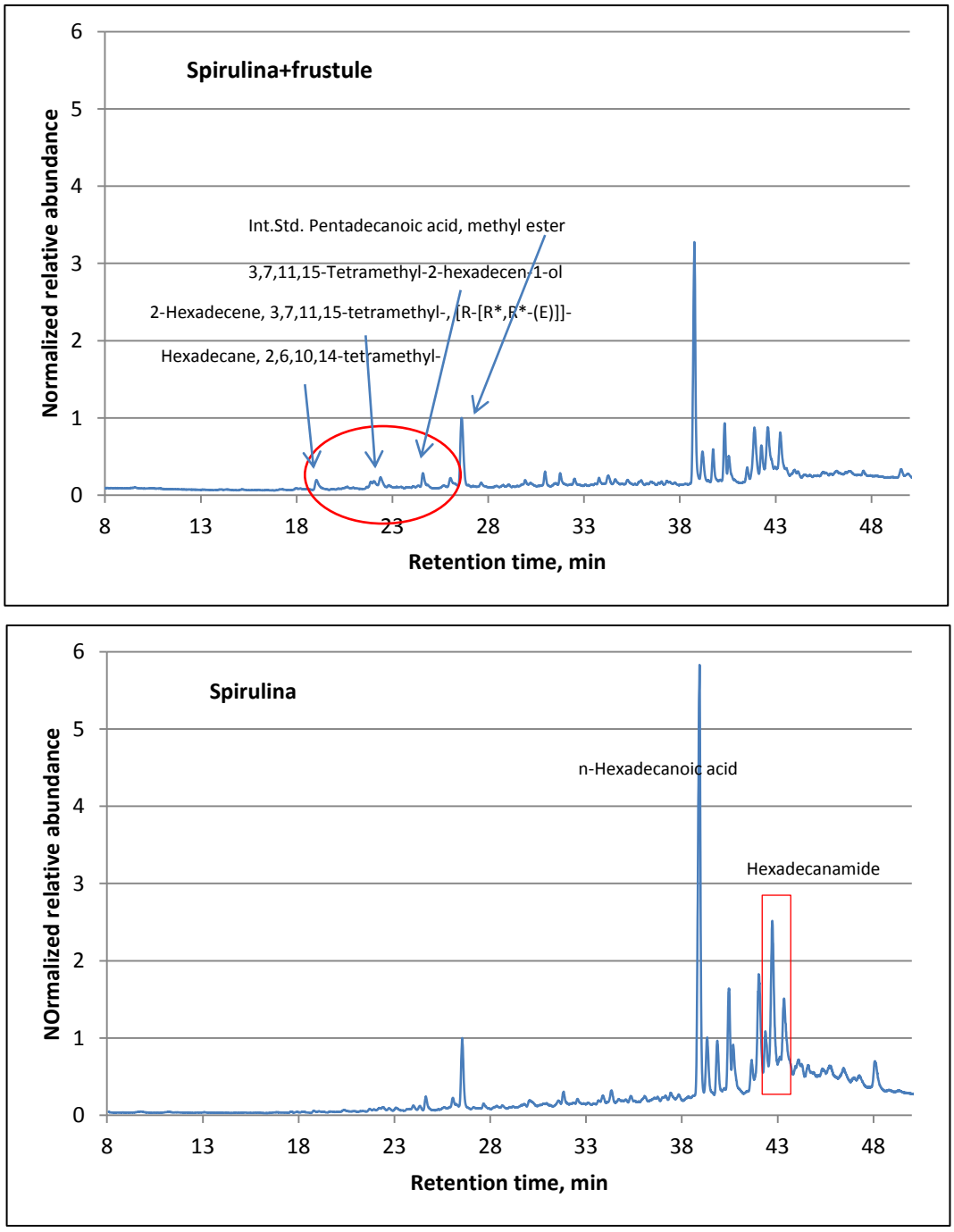

Figure 4.5 Normalized GC spectra of bio crude oil from *Spirulina* and frustule mixture, and (b) *Spirulina* at 300C and 60min HTL tests

Alkanes and Fatty acids/derivatives all together comprised over 80% of identified compounds. After proper separation process, alkanes from diatom bio crude oil (C6-C14) can be used easily as gasoline (commonly C4-C12). Fatty acids/derivatives could be used fairly easily as well through transesterification as bio-diesel or thermal cracking to get more alkanes.

4.4. SEM and FT-IR Characterization

As there was a significant amount of ash in the diatom feedstock due to the frustules, SEM and FT-IR were used to help with the illustration of the possible influence of this unique structure of diatoms after hydrothermal treatment. FT-IR was used as a complimentary method to explain the chemical information on the frustules.

Under SEM, we found dominance of *S. costatum* frustules but also considerable counts of *Nitzschia sp.* as described in previous Chapter. Figure 4.6 shows the diatoms morphology in different existence forms, namely, as feedstock (a), ash (b), raw oil (c), and solid residue (d). In the SEM image of diatom feedstock, we can see the frustules are already in pieces prior to hydrothermal treatment. This is probably due to the harvesting and drying process as high speed centrifuge was used to harvest the algae paste, and followed by grinding. The mechanic abrasion is the cause of the breaking frustules. Other than frustules, which are of fine detailed on the surface, we can also see some amorphous substances on frustules or beside them. Those substances are most like to be the organic matters in diatoms themselves by comparison with the SEM image of ash (b). The image of ash shows a majority of frustules in pieces and they are without the amorphous substances, as they were eventually burned. Also we can see that even under the temperature of 600°C for hours (ash), the fine details of frustules still remained, which

means they are extremely resistant to heat. Images c and d are of raw oil and solid residue. It is obvious that raw oil is more heavily covered by the amorphous substances than solid residue is. As mentioned before, the solid residue is the substance after Soxhlet extraction of raw oil. Thus it is reasonable to assume that the amorphous substances in these images are the converted biomass. Furthermore, we may assume all the bio crude oil was completely extracted from raw oil, thus the amorphous substances on the solid residue may be bio char.

On the other hand, FT-IR spectra can tell the bulk chemical properties such as functional groups that can help us extrapolate the chemical compounds on the solid surfaces. To begin with, the ash content showed two major absorption peaks: one at around 3400 cm^{-1}, the other from 900-1200 cm^{-1}. These two peaks correspond to H-O stretching, and the characteristic band of the existence of silica. H-O stretching may be a result of the water in the ash (as moisture) or possibly from hydroxide (e.g. KOH), and of course SiO_2 is predominant as the ash is full of frustules. However, the spectrum for diatom feedstock is extremely complicated. As we see from its chemical composition, there are proteins, carbohydrates, lipids, etc. in diatom biomass. Thus, we expect to see functional groups such as C=O, C-NH_2, -CH_3, -CH2, O-H, N-H. Absorption of some functional groups may overlap and thus may result in unusually broad peaks. In the spectrum, we can see there is a very wide absorption ranging from about 3700 cm^{-1} to 2700cm^{-1}, which reveals X-H bond. Characteristic absorption of O-H stretching and N-H stretching are at 3600 cm^{-1} to 3000 cm^{-1}. There are two split peaks at 3000 cm^{-1} to 2900 cm^{-1}, featuring aliphatic C-H stretching. And around 3000 cm^{-1} it represents aromatic C-H stretching. Starting from 1700 cm^{-1}, there is another region with several peaks. The

peak at 1700 cm^{-1} to 1600 cm^{-1} features carboxyl group (C=O stretching), which is abundant in the biomass due to presence of protein and lipid. Peak around 1500 cm^{-1} may be due to C=C double bond stretching. Peaks around 1400 cm^{-1} are another characteristic for aliphatic C-H bond (bending). The last wide peak, which is the same as in ash, is for SiO_2. Thus all the possible functional groups were found in FT-IR spectrum of diatom feedstock.

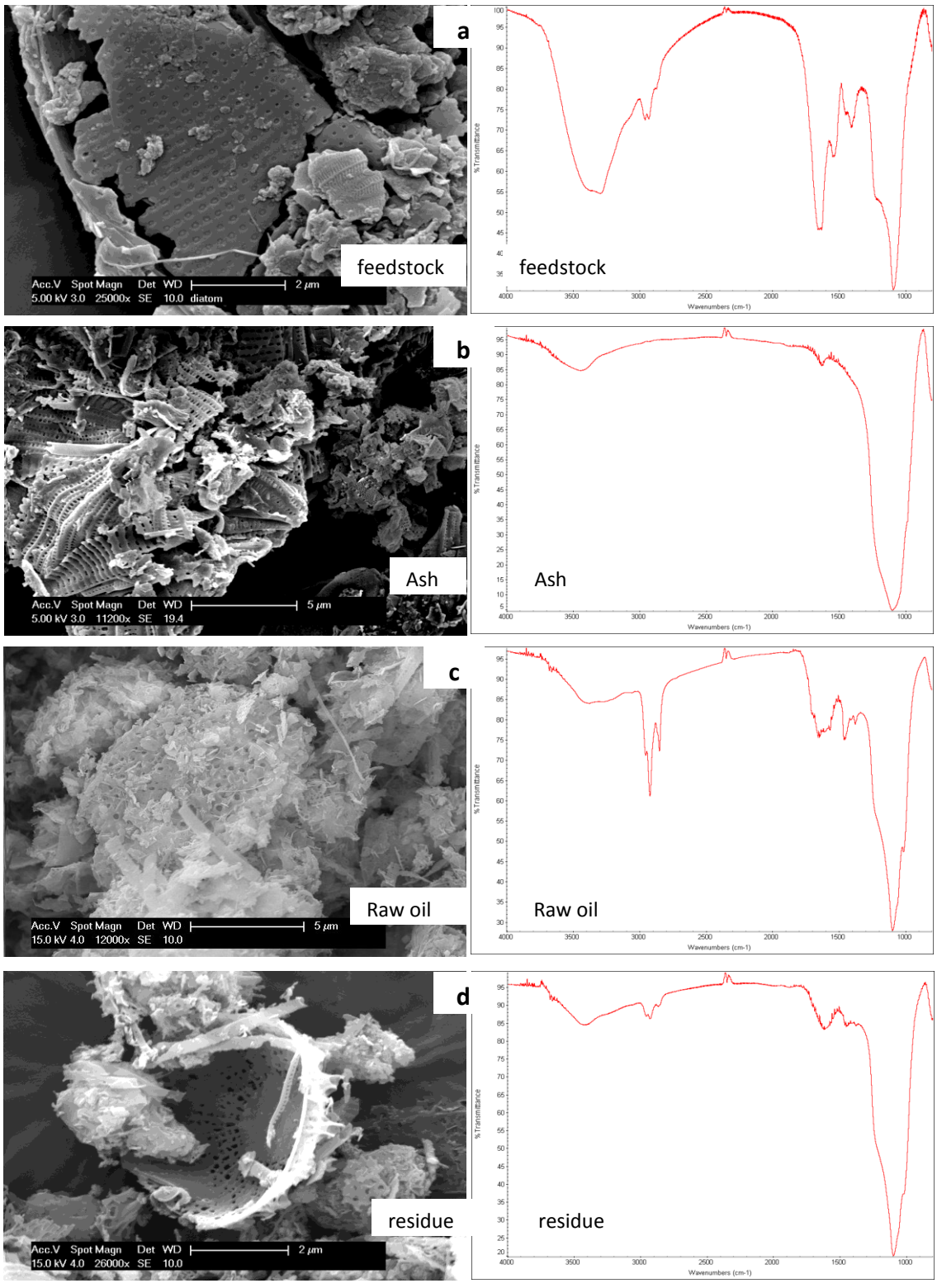

Figure 4.6 SEM images and corresponding FT-IR spectrum of diatom feedstock after different treatment: (a) SEM image and FT-IR spectrum of diatom feedstock (untreated); (b) SEM image and FT-IR spectrum of ash (high temperature treated); SEM images and FT-IR spectra of raw oil (c) and solid residue (d) after 320°C 90min hydrothermal treatment.

After hydrothermal treatment under 320°C and 90min, organic matters in diatoms were converted into bio crude oil and bio char. From the FT-IR spectrum of raw oil, we found that there is a very obvious reduction of peaks. The huge peak at 3600 - 3000 cm^{-1} that appeared in feedstock has greatly shrunken. This means there was a significant decrease in the amount of X-H bond, such as O-H and N-H. This result is reasonable as we expect carbohydrate (which features O-H bond) and protein (which features N-H bond) to be converted into oily compounds. On the other hand, peaks at 3000 cm^{-1} – 2900 cm^{-1} are more obvious as the amount of aliphatic C-H bond has been improved also due to the increased amount of oily compounds. The peaks at 1700 - 1600 cm^{-1} representing carboxyl group has also decreased as the protein has undergone decarboxylation reactions and released carboxyl groups as CO_2 to the gas phase. FT-IR spectrum of solid residue is very similar to that of raw oil, but only shows much weaker intensity.

It is certainly worth noting that the organic matters that remain in the residue can most likely explain whether or not there is any interaction between silica frustules and the organic materials mentioned earlier that might possibly catalyze and enhance the yield and quality of bio crude oil compared with other microalgae. However, limited by the available analytical methods and time, we were not able to delve into this sub-topic.

Chapter 5

Conclusions and Recommendations

5.1. Conclusions

In this study we showed the potential of diatoms as feedstock to produce biofuel via hydrothermal process. The hydrothermal liquefaction products from diatoms are quite different from those of other microalgae species, because of their unique physical properties and chemical composition. This is possibly because of the presence of silica frustules.

The hydrothermal liquefied products of diatoms occur in three phases, namely, gaseous products, solid products (raw oil), and aqueous products. The bio crude oil is absorbed in the solid products, thus further extraction is needed to separate it from the solid residue, which is mainly frustules from diatom cells themselves.

Bio crude oil yield is between 13% (d.w.t.) to 36% (d.w.t.). The highest yield was 35.6% (d.w.t.) at 320°C and 75 min. The lowest yield was 12.95% at 260°C and 75 min. However if we subtract the ash content (which is up to 39% d.w.t.) and only count in the volatile substance, the yield will be between 21% (v.w.t.) and 59% (v.w.t.). This yield is comparably high if ash content is excluded.

The heating values of several selected samples were between 28 MJ/kg to 32.83 MJ/kg. All bio crude oil samples showed a concentrated energy density compared to diatom feedstock with the heating value of 19.18 MJ/kg.

The quality of bio crude oil from diatoms is relatively better than that from other high protein microalgae species because of high yield of alkanes and fatty acyls, as well

as low yield of nitrogen-containing hetero-aromatics. This indicates that upgrading of diatom bio crude oil may be easier, if it is able to separate them properly.

There is still a great amount of solid residue after hydrothermal liquefaction. The solid residue is composed primarily of frustules, which take the form of a rather rigid silica shell. In a set of primary tests, the frustules seemed to help the conversion of the fatty acid/derivatives to similar alkanes, which improves the oil quality. However, the existence of this amount of solid residue may also cause problem when considering industrialize biofuel production with diatoms as feedstock, due to clogging. Also, phase and product separation may cause a considerable amount of additional costs. There is still some organic residue left on its surface according to analyses. This may indicate char formation.

5.2. Recommendations

This study thus provides a useful yet limited amount of information regarding to biofuel production using diatoms as feedstock via hydrothermal liquefaction. Nevertheless, there still remains much to be explored in the quest to determine whether or not diatoms may serve as a potential feedstock for biofuels, or even better than other species of microalgae.

As the diatom feedstock was not pretreated prior to hydrothermal liquefaction, there is one question of whether there is a way to “wash off” the organic biomass from the frustules. As we have seen in SEM image that most frustules were broken, thus this pretreatment might be feasible. However, this may introduce another problem of whether or not this pretreatment would introduce another variable to the bio crude oil yield and its

chemical composition. On the other hand, this pretreatment of separating frustules may be critical for scale-up.

Study of how proteins can be converted into fatty acyls is crucial in the case of using high protein microalgae. As microalgae produce lipids under environmental stress which usually associates with low biomass production, it might be more efficient to use high protein microalgae once we know this pathway.

As the bio crude oil yield of diatom feedstock is comparatively high, and the products are very similar under different hydrothermal conditions. Thus there is a need to investigate the possibility that the frustules might have participated in the reactions and improved the yield of bio crude oil.

The bio crude oil obtained is not a practical transportation fuel to date yet. Thus a routine of upgrading the bio crude oil is essential to put this product in use. With low nitrogen-containing hetero-aromatics content and high alkanes and fatty acyls, it is possible to directly adopt hydrotreating and hydrocracking in lab scale to evaluate its cost-efficiency.

References

Akhtar, J. and N. A. S. Amin. 2011. A review on process conditions for optimum bio-oil yield in hydrothermal liquefaction of biomass. *Renewable and Sustainable Energy Reviews* 15(3): 1615-1624.

Anastasakis, K. and A. B. Ross. 2011. Hydrothermal liquefaction of the brown macro-alga Laminaria Saccharina: Effect of reaction conditions on product distribution and composition. *Bioresource technology* 102(7): 4876-4883.

Bandura, A. V. and S. N. Lvov. 2006. The ionization constant of water over wide ranges of temperature and density. *Journal of physical and chemical reference data* 35(1): 15-30.

Bentley, R. and G. Boyle. 2008. Global oil production: forecasts and methodologies. *Environment and Planning B Planning And Design* 35(4): 609.

Bentley, R. W. 2002. Global oil & gas depletion: an overview. *Energy Policy* 30(3): 189-205.

Biller, P. and A. B. Ross. 2011. Potential yields and properties of oil from the hydrothermal liquefaction of microalgae with different biochemical content. *Bioresource technology* 102(1): 215-225.

Birol, F. and M. Argiri. 1999. World energy prospects to 2020. *Energy* 24(11): 905-918.

Brown, T. M., P. Duan and P. E. Savage. 2010. Hydrothermal Liquefaction and Gasification of Nannochloropsis sp. *Energy & Fuels* 24(6): 3639-3646.

Chisti, Y. 2007. Biodiesel from microalgae. *Biotechnology Advances* 25(3): 294-306.

Compton, J. C. 2010. *Diatoms: ecology and life cycle.* New York: Nova Science Publishers, Inc.

De Bari, I., F. Nanna and G. Braccio. 2007. SO2-catalyzed steam fractionation of aspen chips for bioethanol production: optimization of the catalyst impregnation. *Industrial & Engineering Chemistry Research* 46(23): 7711-7720.

Dismukes, G. C., D. Carrieri, N. Bennette, G. M. Ananyev and M. C. Posewitz. 2008. Aquatic phototrophs: efficient alternatives to land-based crops for biofuels. *Current opinion in biotechnology* 19(3): 235-240.

Donner, S. D. and C. J. Kucharik. 2008. Corn-based ethanol production compromises goal of reducing nitrogen export by the Mississippi River. *Proceedings of the National Academy of Sciences* 105(11): 4513-4518.

Dote, Y., S. Inoue, T. Ogi and S. Yokoyama. 1998. Distribution of nitrogen to oil products from liquefaction of amino acids. *Bioresource technology* 64(2): 157-160.

Dote, Y., S. Sawayama, S. Inoue, T. Minowa and S. Yokoyama. 1994. Recovery of Liquid Fuel from Hydrocarbon-Rich Microalgae by Thermochemical Liquefaction. *Fuel* 73(12): 1855-1857.

Dote, Y., S. Inoue, T. Ogi and S. Yokoyama. 1996. Studies on the direct liquefaction of protein-contained biomass: The distribution of nitrogen in the products. *Biomass and Bioenergy* 11(6): 491-498.

Duan, P. and P. E. Savage. 2010. Hydrothermal liquefaction of a microalga with heterogeneous catalysts. *Industrial & Engineering Chemistry Research* 50(1): 52-61.

EIA. 2012. **Annual Energy Outlook 2012** with Projections to 2035. 2012.

Escobar, J. C., E. S. Lora, O. J. Venturini, E. E. Yáñez, E. F. Castillo and O. Almazan. 2009. Biofuels: environment, technology and food security. *Renewable and sustainable energy reviews* 13(6): 1275-1287.

Falkowski, P. G. and A. H. Knoll. 2007. *Evolution of primary producers in the sea.* MA: Elsevier Academic Press.

Falkowski, P. G., M. E. Katz, A. H. Knoll, A. Quigg, J. A. Raven, O. Schofield and F. Taylor. 2004. The evolution of modern eukaryotic phytoplankton. *Science* 305(5682): 354-360.

Fernandez, F., F. G. Camacho, J. Perez, J. Sevilla and E. M. Grima. 1998. Modeling of biomass productivity in tubular photobioreactors for microalgal cultures: effects of dilution rate, tube diameter, and solar irradiance. *Biotechnology and bioengineering* 58(6): 605-616.

Field, C. B., M. J. Behrenfeld, J. T. Randerson and P. Falkowski. 1998. Primary production of the biosphere: integrating terrestrial and oceanic components. *Science* 281(5374): 237-240.

Fischer, G. 2002. Global agro-ecological assessment for agriculture in the 21st century: methodology and results.

Fu, J., F. Shi, L. Thompson Jr, X. Lu and P. E. Savage. 2011. Activated carbons for hydrothermal decarboxylation of fatty acids. *Acs Catalysis* 1(3): 227-231.

Goldemberg, J., S. T. Coelho and P. Guardabassi. 2008. The sustainability of ethanol production from sugarcane. *Energy Policy* 36(6): 2086-2097.

Ho, T. and D. Subba Rao. 2006. The trace metal composition of marine microalgae in cultures and natural assemblages. *Algal cultures, analogues of blooms and applications, Volume 1*271-299.

Holliday, R. L., J. W. King and G. R. List. 1997. Hydrolysis of vegetable oils in sub-and supercritical water. *Industrial & Engineering Chemistry Research* 36(3): 932-935.

Höök, M., R. Hirsch and K. Aleklett. 2009. Giant oil field decline rates and their influence on world oil production. *Energy Policy* 37(6): 2262-2272.

Huber, G. W., S. Iborra and A. Corma. 2006. Synthesis of transportation fuels from biomass: chemistry, catalysts, and engineering. *Chemical reviews* 1064044-4098.

Huntley, M. E. and D. G. Redalje. 2007. CO2 mitigation and renewable oil from photosynthetic microbes: a new appraisal. *Mitigation and Adaptation Strategies for Global Change* 12(4): 573-608.

IEA. 2012. *Key World Energy Statistics 2012.* 2012th ed. Paris: International Energy Agency.

Isichei, A. O. 1990. The role of algae and cyanobacteria in arid lands. A review. *Arid Land Research and Management* 4(1): 1-17.

Jena, U., K. Das and J. Kastner. 2012. Comparison of the effects of Na2CO3, Ca3 (PO4) 2, and NiO catalysts on the thermochemical liquefaction of microalga Spirulina platensis. *Applied Energy* 98368-375.

Jena, U., K. Das and J. Kastner. 2011. Effect of operating conditions of thermochemical liquefaction on biocrude production from Spirulina platensis. *Bioresource technology* 102(10): 6221-6229.

Johansen, M. N. 2011. *Microalgae: biotechnology, microbiology, and energy.* New York: Nova Science Publishers, Inc.

Karagöz, S., T. Bhaskar, A. Muto and Y. Sakata. 2006. Hydrothermal upgrading of biomass: Effect of K₂CO₃concentration and biomass/water ratio on products distribution. *Bioresource technology* 97(1): 90-98.

Karagöz, S., T. Bhaskar, A. Muto and Y. Sakata. 2005. Catalytic hydrothermal treatment of pine wood biomass: effect of RbOH and CsOH on product distribution. *Journal of Chemical Technology and Biotechnology* 80(10): 1097-1102.

Kawamoto, H., S. Saito, W. Hatanaka and S. Saka. 2007. Catalytic pyrolysis of cellulose in sulfolane with some acidic catalysts. *Journal of Wood Science* 53(2): 127-133.

Kheshgi, H. S., R. C. Prince and G. Marland. 2000. The Potential of Biomass Fuels in The Context of Global Climate Change: Focus on Transportation Fuels 1. *Annual Review of Energy and the Environment* 25(1): 199-244.

Klass, D. L. 1998. *Biomass for renewable energy, fuels, and chemicals.* Academic press.

Klingler, D., J. Berg and H. Vogel. 2007. Hydrothermal reactions of alanine and glycine in sub-and supercritical water. *The Journal of Supercritical Fluids* 43(1): 112-119.

Kruse, A., P. Maniam and F. Spieler. 2007. Influence of proteins on the hydrothermal gasification and liquefaction of biomass. 2. Model compounds. *Industrial & Engineering Chemistry Research* 46(1): 87-96.

Kruse, A., A. Krupka, V. Schwarzkopf, C. Gamard and T. Henningsen. 2005. Influence of proteins on the hydrothermal gasification and liquefaction of biomass. 1. Comparison of different feedstocks. *Industrial & Engineering Chemistry Research* 44(9): 3013-3020.

Lardon, L., A. Hélias, B. Sialve, J. Steyer and O. Bernard. 2009. Life-cycle assessment of biodiesel production from microalgae. *Environmental science & technology* 43(17): 6475-6481.

Liu, A., Y. Park, Z. Huang, B. Wang, R. O. Ankumah and P. K. Biswas. 2006. Product identification and distribution from hydrothermal conversion of walnut shells. *Energy & Fuels* 20(2): 446-454.

Lu, Q., W. Xiong, W. Li, Q. Guo and X. Zhu. 2009. Catalytic pyrolysis of cellulose with sulfated metal oxides: a promising method for obtaining high yield of light furan compounds. *Bioresource technology* 100(20): 4871-4876.

Macedo, I. C., J. E. Seabra and J. E. Silva. 2008. Green house gases emissions in the production and use of ethanol from sugarcane in Brazil: The 2005/2006 averages and a prediction for 2020. *Biomass and Bioenergy* 32(7): 582-595.

Moheimani, N. R. and M. A. Borowitzka. 2006. The long-term culture of the coccolithophore Pleurochrysis carterae (Haptophyta) in outdoor raceway ponds. *Journal of Applied Phycology* 18(6): 703-712.

Ogata, Y., E. Imai, H. Honda, K. Hatori and K. Matsuno. 2000. Hydrothermal circulation of seawater through hot vents and contribution of interface chemistry to prebiotic synthesis. *Origins of Life and Evolution of the Biosphere* 30(6): 527-537.

Parsons, T., K. Stephens and J. Strickland. 1961. On the chemical composition of eleven species of marine phytoplankters. *Journal of the Fisheries Board of Canada* 18(6): 1001-1016.

Pérez, J., J. Munoz-Dorado, T. de la Rubia and J. Martinez. 2002. Biodegradation and biological treatments of cellulose, hemicellulose and lignin: an overview. *International Microbiology* 5(2): 53-63.

Petersen, M. Ø, J. Larsen and M. H. Thomsen. 2009. Optimization of hydrothermal pretreatment of wheat straw for production of bioethanol at low water consumption without addition of chemicals. *Biomass and Bioenergy* 33(5): 834-840.

Peterson, A. A., F. Vogel, R. P. Lachance, M. Fröling, M. J. Antal Jr and J. W. Tester. 2008. Thermochemical biofuel production in hydrothermal media: A review of sub-and supercritical water technologies. *Energy Environ.Sci.* 1(1): 32-65.

Radmer, R. J. 1996. Algal diversity and commercial algal products. *Bioscience* 46(4): 263-270.

Reinfelder, J. R., A. J. Milligan and F. M. Morel. 2004. The role of the C4 pathway in carbon accumulation and fixation in a marine diatom. *Plant Physiology* 135(4): 2106-2111.

Ross, A., P. Biller, M. Kubacki, H. Li, A. Lea-Langton and J. Jones. 2010. Hydrothermal processing of microalgae using alkali and organic acids. *Fuel* 89(9): 2234-2243.

Sato, N., A. T. Quitain, K. Kang, H. Daimon and K. Fujie. 2004. Reaction kinetics of amino acid decomposition in high-temperature and high-pressure water. *Industrial & Engineering Chemistry Research* 43(13): 3217-3222.

Sheehan, J., T. Dunahay, J. Benemann and P. Roessler. 1998. *A look back at the US department of energy's aquatic species program: biodiesel from algae.* National Renewable Energy Laboratory Golden, CO.

Simoneit, B. R. 1993. Aqueous high-temperature and high-pressure organic geochemistry of hydrothermal vent systems. *Geochimica et Cosmochimica Acta* 57(14): 3231-3243.

Sperling, D. and D. Gordon. 2009. *Two billion cars: driving toward sustainability.* Oxford University Press, USA.

Sun, Y. and J. Cheng. 2002. Hydrolysis of lignocellulosic materials for ethanol production: a review. *Bioresource technology* 83(1): 1-11.

Taherzadeh, M. J. and K. Karimi. 2008. Pretreatment of lignocellulosic wastes to improve ethanol and biogas production: a review. *International Journal of Molecular Sciences* 9(9): 1621-1651.

Tekin, K., S. Karagöz and S. Bektaş. 2013. Effect of sodium perborate monohydrate concentrations on product distributions from the hydrothermal liquefaction of Scotch pine wood. *Fuel Processing Technology* 11017-23.

Tjeerdsma, B. and H. Militz. 2005. Chemical changes in hydrothermal treated wood: FTIR analysis of combined hydrothermal and dry heat-treated wood. *Holz als Roh-und Werkstoff* 63(2): 102-111.

Tozzi, S., O. Schofield and P. Falkowski. 2004. Historical climate change and ocean turbulence as selective agents for two key phytoplankton functional groups. *Marine Ecology Progress Series* 274123-132.

Vardon, D. R., B. Sharma, J. Scott, G. Yu, Z. Wang, L. Schideman, Y. Zhang and T. J. Strathmann. 2011. Chemical properties of biocrude oil from the hydrothermal

liquefaction of Spirulina algae, swine manure, and digested anaerobic sludge. *Bioresource technology* 102(17): 8295-8303.

Wang, Z. 2011. Reaction mechanisms of hydrothermal liquefaction of model compounds and biowaste feedstocks. PhD diss. University of Illinois at Urbana-Champaign.

Watanabe, M., T. Iida and H. Inomata. 2006. Decomposition of a long chain saturated fatty acid with some additives in hot compressed water. *Energy conversion and management* 47(18): 3344-3350.

Weyer, K. M., D. R. Bush, A. Darzins and B. D. Willson. 2010. Theoretical maximum algal oil production. *BioEnergy Research* 3(2): 204-213.

Williams, P. J. and L. M. Laurens. 2010. Microalgae as biodiesel & biomass feedstocks: Review & analysis of the biochemistry, energetics & economics. *Energy & Environmental Science* 3(5): 554-590.

Yang, H., R. Yan, H. Chen, D. H. Lee and C. Zheng. 2007. Characteristics of hemicellulose, cellulose and lignin pyrolysis. *Fuel* 86(12): 1781-1788.

Yang, Y., C. Feng, Y. Inamori and T. Maekawa. 2004. Analysis of energy conversion characteristics in liquefaction of algae. *Resources, Conservation and Recycling* 43(1): 21-33.

Yu, G. 2012. Hydrothermal liquefaction of low-lipid microalgae to produce bio-crude oil. PhD diss. Urbana, IL: University of Illinois at Urbana-Champaign.

Yu, G., Y. Zhang, L. Schideman, T. Funk and Z. Wang. 2011. Distributions of carbon and nitrogen in the products from hydrothermal liquefaction of low-lipid microalgae. *Energy & Environmental Science* 4(11): 4587-4595.

Zeng, M., N. S. Mosier, C. Huang, D. M. Sherman and M. R. Ladisch. 2007. Microscopic examination of changes of plant cell structure in corn stover due to hot water pretreatment and enzymatic hydrolysis. *Biotechnology and bioengineering* 97(2): 265-278.

Zhang, B., M. von Keitz and K. Valentas. 2008. Thermal effects on hydrothermal biomass liquefaction. *Applied Biochemistry and Biotechnology* 147(1-3): 143-150.

Zhou, C. H., X. Xia, C. X. Lin, D. S. Tong and J. Beltramini. 2011. Catalytic conversion of lignocellulosic biomass to fine chemicals and fuels. *Chemical Society Reviews* 40(11): 5588-5617.

Zhu, X., S. P. Long and D. R. Ort. 2008. What is the maximum efficiency with which photosynthesis can convert solar energy into biomass? *Current opinion in biotechnology* 19(2): 153-159.

Zou, S., Y. Wu, M. Yang, C. Li and J. Tong. 2009. Thermochemical catalytic liquefaction of the marine microalgae Dunaliella tertiolecta and characterization of bio-oils. *Energy & Fuels* 23(7): 3753-3758.